LINEAR STABILITY OF FLOW IN A CONCENTRIC ANNULUS

By
ANIL K. AGARWAL

DEPARTMENT OF MECHANICAL ENGINEERING
INDIAN INSTITUTE OF TECHNOLOGY KANPUR
FEBRUARY, 1976

LINEAR STABILITY OF FLOW IN A CONCENTRIC ANNULUS

A Thesis Submitted
in partial Fulfilment of the Requirements
for the Degree of
MASTER OF TECHNOLOGY

By
ANIL K. AGARWAL

to the

DEPARTMENT OF MECHANICAL ENGINEERING
INDIAN INSTITUTE OF TECHNOLOGY KANPUR
FEBRUARY, 1976

Dedicated

to my

Reverend Parents

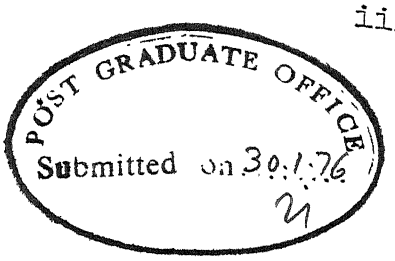

CERTIFICATE

This is to certify that this work on 'Linear Stability of Flow in a Concentric Annulus' has been carried out under my supervision and has not been submitted elsewhere for a degree.

V.K. Garg
Assistant Professor
Department of Mechanical Engineering
Indian Institute of Technology Kanpur

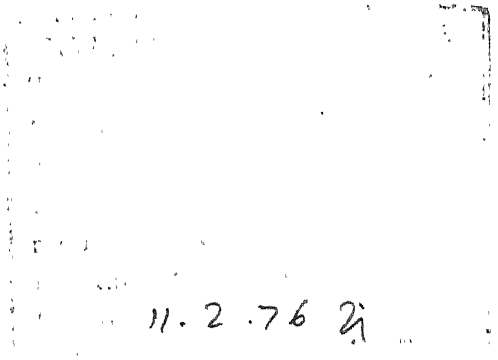

ACKNOWLEDGEMENTS

I take this opportunity to express a deep sense of gratitude and appreciation towards Professor Vijay K. Garg of the Department of Mechanical Engineering for his able guidance and keen interest throughout the investigation.

I also extend my sincere thanks to Shri S. Kapoor, of Computer Center, and to Shri A.K. Bajaj, of the Mechanical Engineering Department, for their continued cooperation and valuable discussions.

My thanks are also due to Shri B.L. Arora for drawing the graphs and Shri J.D. Verma for a careful typing.

Anil K. Agarwal

TABLE OF CONTENTS

LIST OF FIGURES

LIST OF TABLES

NOMENCLATURE

a,b,c and d	exponent of (1-r) defined by equations (3.3) through (3.6)
C	a closed contour in the complex k or ω- plane
C_1	a closed contour in the complex determinant plane
C_m	the m^{th} coefficient in the series expansion for the steady basic velocity (equation (3.1))
C_p	phase velocity of a mode
det	determinant defined by equation (3.31)
D	the operator $\frac{d}{dr}$, $\frac{d}{dz}$ or $\frac{d}{dx}$
e	the exponential function
$\underset{\sim}{e}_r$, $\underset{\sim}{e}_\theta$ and $\underset{\sim}{e}_z$	unit vectors in the radial, circumferential and axial direction respectively
f	complex function of a complex variable z; function of dependent and independent variables in a differential equation
h	step size for integration
i	$\sqrt{-1}$
k	dimensionless complex wave number
k*	dimensional counterpart of k
k_i	the imaginary part of k
k_m	the m^{th} value of k (equation (1.5))
k_r	the real part of k
K, K_1, K_2, K_3, K_4 and K'	variables used in Appendix I
m	a positive integer

M	number of eigenvalues enclosed by a certain region in the complex k or ω -plane
n	the azimuthal mode number
p	dimensionless perturbation pressure
p^*	dimensional perturbation pressure
$\bar{p}$	complex eigenfunction for perturbation pressure
P	resultant pressure in the flow (see equation 2.2)); number of poles of f(z) within a closed region C
P_m	the m^{th} coefficient in the series expansion for $\bar{p}$ (equation (3.6))
$\bar{P}^*$	steady mean pressure (equation (2.2))
r	radial coordinate (synonymous with r' from equation (2.15) onwards)
r'	dimensionless radial coordinate
r_1	inner radius of the annulus
r_2	outer radius of the annulus
r_s	radius up to which the series solution is carried
R	modified Reynolds number (equation (2.13))
R_a	actual Reynolds number
Re (z)	denotes the real part of a complex number z
s	any exponent of (1-r)
t	time (synonymous with t' from equation (2.15) onwards)

t'	dimensionless time
U_m	the m^{th} coefficient in the series expansion for $\bar{v}_z$ (equation (3.5))
v_r, v_θ and v_z	dimensionless radial, circumferential and axial components of disturbance velocity
$\underset{\sim}{v}^*$	disturbance velocity vector whose components are v_r^*, v_θ^* and v_z^*
v_r^*, v_θ^* and v_z^*	dimensional counterparts of v_r, v_θ and v_z respectively
$\bar{v}_r$, $\bar{v}_\theta$ and $\bar{v}_z$	complex eigenfunctions for v_r, v_θ and v_z respectively
$\hat{\underset{\sim}{v}}$	complex vector whose real parts are v_r^*, v_θ^* and v_z^*
$\underset{\sim}{v}_n$	vector defined by equation (1.1)
$\tilde{\underset{\sim}{v}}_{nm}$	vector defined by equation (1.2)
$\bar{\underset{\sim}{v}}_{nm}$	vector defined by equation (1.3)
$\tilde{\tilde{\underset{\sim}{v}}}_{nm}$	vector defined by equation (1.5)
$\bar{\tilde{\underset{\sim}{v}}}_{nm}$	vector defined by equation (1.6)
$\bar{V}_r^*$, $\bar{V}_\theta^*$ and $\bar{V}_z^*$	radial, circumferential and axial components of the dimensional steady basic velocity
$\bar{\underset{\sim}{V}}^*$	dimensional steady basic velocity whose components are $\bar{V}_r^*$, $\bar{V}_\theta^*$ and $\bar{V}_z^*$
V_{av}	average, over the flow cross-section, of $\bar{V}_z^*$

$\bar{V}_z$	dimensionless basic flow velocity
V_r, V_θ and V_z	radial, circumferential and axial components of the total flow velocity
$\underset{\sim}{V}$	total velocity vector
V_m	the m^{th} coefficient in the series expansion for $\bar{v}_r$ (equation (3.3))
W_m	the m^{th} coefficient in the series expansion for $i\bar{v}_\theta$ (equation (3.4))
x	real part of the complex variable z; independent variable in a differential equation
X	real part of the complex function f(z)
y	imaginary part of the complex variable z; dependent variable in a differential equation
Y	imaginary part of the complex function f(z)
z	axial coordinate (synonymous with z' from equation (2.15) onwards); complex variable as in Appendix II
z'	dimensionless axial coordinate
Z	number of zeros of f(z) within a closed region C
α	variable defined in equation (2.14)
β	variable defined in equation (2.14)
γ	diameter or radius ratio (r_1/r_2)
θ	angular coordinate
ν	kinematic viscosity of the fluid
π	the constant 3.14159...
ω	dimensionless complex frequency

ω^*	dimensional counterpart of ω
ρ	density of the incompressible fluid
ϕ	any dimensionless quantity used as dummy for v_r, v_θ, v_z or p
$\hat{\phi}$	complex quantity whose real part is ϕ
$\overline{\phi}$	function defined by equation (2.19)
$\underset{\sim}{0}$	null vector
$\sum_{j=1}^{m}$	summation over j from 1 to m
i.e.	that is
cf.	compare from
$\lvert \quad \rvert$	absolute value
e.g.	for example

ABSTRACT

A theoretical study of the linear stability (both temporal and spatial) of flow in a rigid, concentric annulus to axisymmetric and non-axisymmetric disturbances is presented here. The continuity and Navier - Stokes equations are reduced to a set of coupled, linear, ordinary differential equations governing the propagation of the disturbance. The flow is said to be temporally stable if the disturbance, applied at an initial instant everywhere in the fluid and periodic in the downstream direction, decays with time while it is considered to be spatially stable if the disturbance, periodic in time and imposed at a specified location, decays in the downstream direction. The coupled differential equations are solved numerically for the complex eigenvalues. The integration starts at the outer wall by means of a Frobenius series and is continued to the inner wall by the fourth order Runge-Kutta method. An eigenvalue search technique is employed to ascertain the number of eigenvalues within a closed region of the complex ω or k-plane. Actual isolation of the eigenvalues is achieved by means of an iterative scheme. Results are presented for the linear spatial stability of the annular flow to axisymmetric disturbances. Three different annuli with diameter ratio γ = 0.2, 0.5 and 0.8 are considered. It is found that the flow is spatially stable to infinitesimal axisymmetric disturbances up to a modified Reynolds number of 10,000.

CHAPTER 1

INTRODUCTION

Numerous efforts have been made to clarify and explain theoretically the remarkable process of transition from laminar to turbulent flow. The recent theoretical investigations are based on the assumption that laminar flows are affected by certain small disturbances; for example, in the case of a boundary layer on a solid-body placed in a stream, these disturbances may be due to wall roughness and/or due to irregularities in the external flow stream, whereas in the case of pipe flow, they may originate in the inlet section. The stability theory endeavours to follow the behaviour of such disturbances, when they are superimposed on the main flow, the decisive question to answer in this respect is whether the disturbances amplify or decay. If the disturbance ultimately decays to zero the flow is said to be stable, but if the disturbance amplifies the flow is said to be unstable. It does not follow, however, that instability leads to turbulent motion.

The behaviour of small disturbances to a flow can be analyzed in two different ways. In the first of these, a disturbance is assumed to be applied at an initial instant everywhere in the fluid and is, in particular,

periodic in the downstream direction. The flow is then said to be 'temporally' stable if the disturbance decays with time and unstable if it grows. In the second approach, it is assumed that a disturbance which is periodic in time is imposed at a specified location in the fluid and propagates downstream. If the disturbance decays in the down-stream direction, the flow is considered to be 'spatially' stable. Though the latter point of view is physically more realistic, almost all effort has been devoted to the former approach since the very inception of the stability theory. A possible reason for this bias is given at the end of this chapter. While the stability of flow in a circular pipe has been analysed extensively [1-5]*, not much attention has been paid to the flow in an annulus. Only the temporal stability of flow in a concentric annulus to infinitesimal axisymmetric disturbances was considered by Mott and Joseph [6].

The purpose of this study is to analyze theoretically the linear stability of viscous, incompressible flow between coaxial, right-circular cylinders. Both axisymmetric and non-axisymmetric disturbances are considered.

---

*Numbers in square parentheses designate references listed at the end of the dissertation.

The corresponding mathematical problem can be expressed as follows:

For time $t < 0$ we suppose that the flow is undisturbed; for $t \geq 0$ one of the following two situations exists:

(i) For temporal stability, a disturbance is assumed to be applied everywhere in the fluid at $t = 0$. This disturbance is periodic in the downstream direction z, and is an arbitrary function of radial and angular coordinates r and θ.

(ii) For spatial stability, a periodic disturbance is imposed at $z = 0$ and at $t = 0$. This disturbance has a frequency ω and is an arbitrary function of r and θ.

The θ-dependence of the disturbance velocity vector $\underset{\sim}{v}^*$ can be expressed as a Fourier series in θ of the form

$$\underset{\sim}{v}^*(r,\theta,z,t) = \mathrm{Re}\left[\hat{\underset{\sim}{v}}(r,\theta,z,t)\right] = \mathrm{Re}\left[\sum_{n=0}^{\infty} \underset{\sim}{v}_n(r,z,t)\, e^{in\theta}\right], \tag{1.1}$$

where n is the azimuthal mode number, Re denotes the real part of a complex function, and $i = \sqrt{-1}$. For $n = 0$, we have an axisymmetric disturbance; for $n = 1$, the perturbations are constant along a simple helix; for $n = 2$, the perturbations are constant along two interwined helices, and so on.

For the (r,z,t) dependence, there are two possible ways of representing $\underset{\sim}{v}_n$ (r,z,t) depending upon the type of stability analysis.

(i) For temporal stability analysis, each $\underset{\sim}{v}_n$ (r,z,t) can be expressed as a Fourier series of the form

$$\underset{\sim}{v}_n (r,z,t) = \sum_{m=1}^{\infty} \tilde{\underset{\sim}{v}}_{nm} (r,z)\, e^{-i\omega_m t}, \qquad (1.2)$$

where ω_m is the complex frequency to be found. Finally, the z-dependence of $\tilde{\underset{\sim}{v}}_{nm}$ (r,z) can be expressed as

$$\tilde{\underset{\sim}{v}}_{nm} (r,z) = \bar{\underset{\sim}{v}}_{nm} (r)\, e^{kz}, \qquad (1.3)$$

where k (an imaginary quantity) is the wave number of the disturbance. Thus, the disturbance velocity vector is given by the double Fourier series as

$$\underset{\sim}{v}^*(r,\theta,z,t) = \mathrm{Re}\left[\sum_{n=0}^{\infty} \sum_{m=1}^{\infty} \bar{\underset{\sim}{v}}_{nm} (r) \exp (kz + in\theta - i\omega_m t)\right]. \qquad (1.4)$$

(ii) For spatial stability analysis, each $\underset{\sim}{v}_n$ (r,z,t) can be expressed as a Fourier series of the form

$$\underset{\sim}{v}_n (r,z,t) = \sum_{m=1}^{\infty} \tilde{\tilde{\underset{\sim}{v}}}_{nm} (r,t)\, e^{k_m z}, \qquad (1.5)$$

where k_m is the complex wave number to be found. Finally, the t-dependence of $\tilde{\tilde{\underset{\sim}{v}}}_{nm}$ (r,t) can be expressed as

$$\tilde{\tilde{\underset{\sim}{v}}}_{nm} (r,t) = \bar{\bar{\underset{\sim}{v}}}_{nm} (r)\, e^{-i\omega t}, \qquad (1.6)$$

where ω is the real frequency of the disturbance. Thus,

the disturbance velocity vector is given by the double Fourier series as

$$\underset{\sim}{v}^*(r,\theta,z,t) = \mathrm{Re}\left[\sum_{n=0}^{\infty}\sum_{m=1}^{\infty} \underset{\sim}{\overline{\overline{v}}}_{nm}(r)\exp\left(k_m z + in\theta - i\omega t\right)\right]. \tag{1.7}$$

Note that $\underset{\sim}{\hat{v}}(r,\theta,z,t)$, $\underset{\sim}{v}_n(r,z,t)$, $\underset{\sim}{\tilde{v}}_{nm}(r,z)$, $\underset{\sim}{\bar{v}}_{nm}(r)$, $\underset{\sim}{\approx}_{nm}(r,t)$ and $\underset{\sim}{\overline{\overline{v}}}_{nm}(r)$ are all complex vectors.

The flow is said to be temporally stable if the imaginary part of the complex frequency $\omega < 0$, while it is said to be spatially stable if the real part of the complex wave number $k < 0$. Another important difference between the two cases is that, because of the continuity equation (see equation (2.20)), the vector eigenfunction $\underset{\sim}{\bar{v}}(r)$ is equivalent to <u>two</u> scalar eigenfunctions for the temporal stability rather than <u>three</u> as in the case of spatial stability. The problem of spatial or convective stability is, therefore, much more complicated than that of temporal stability, which is quite likely the reason why it has been neglected in the past in favour of temporal studies.

CHAPTER 2

THEORETICAL ANALYSIS

2.1 Mathematical Formulation

It has already been pointed out that the stability of a flow is determined by assuming small disturbances superimposed on the basic flow. Therefore, denoting the basic flow velocity vector by $\underset{\sim}{\overline{V}}^*$ and the disturbance velocity vector by $\underset{\sim}{v}^*$, we can write the total velocity vector $\underset{\sim}{V}$ as

$$\underset{\sim}{V} = \underset{\sim}{\overline{V}}^* + \underset{\sim}{v}^* , \tag{2.1}$$

and similarly the total pressure P as

$$P = \overline{P}^* + p^* . \tag{2.2}$$

Since we are considering the stability of laminar flow between two coaxial, right-circular cylinders, the basic flow has only an axial component of velocity and this component is only a function of the inner and outer radii of the annulus, i.e. $\underset{\sim}{\overline{V}}^* = \overline{V}_z^* (r)\, \underset{\sim}{e}_z$. Other principal assumptions for the analysis to follow are

(i) Incompressible, Newtonian fluid with constant coefficient of viscosity,

(ii) No body forces,

(iii) Steady basic flow,

(iv) Infinitesimal disturbances,

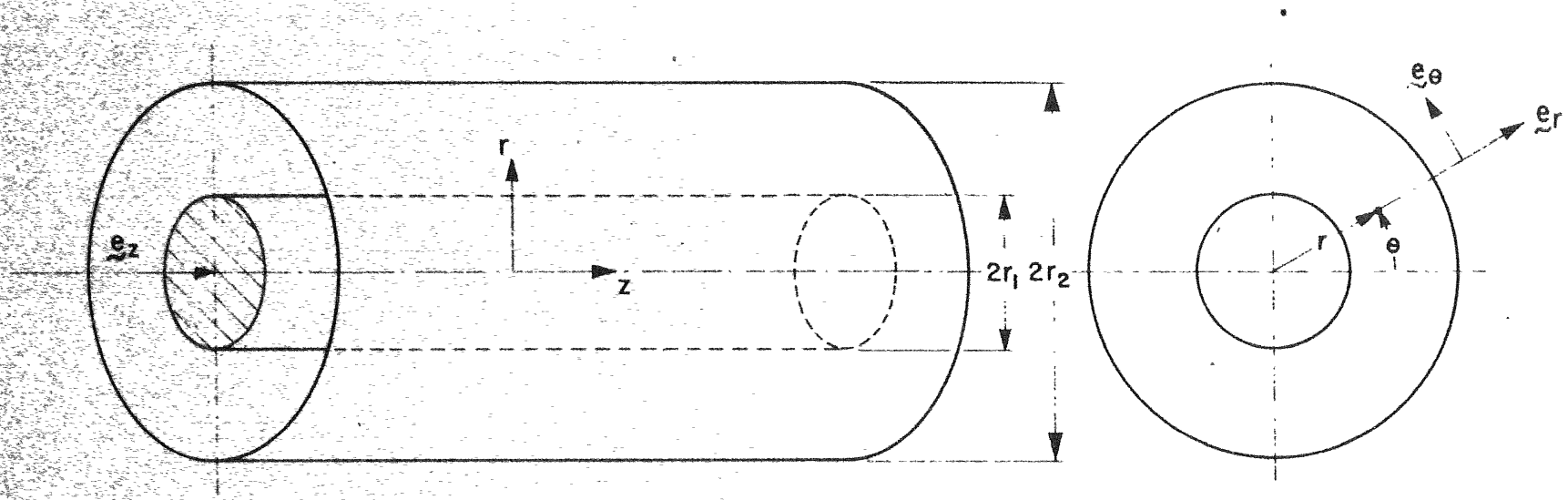

Figure 2.1 Cylindrical Coordinates for the Coaxial Cylinders.

(v) Rigid, Impermeable cylinders,

(vi) No slip at the cylinder walls.

For such a fluid, the equations of motion in cylindrical coordinates (figure 2.1) are

Continuity:

$$\frac{\partial V_r}{\partial r} + \frac{V_r}{r} + \frac{1}{r}\frac{\partial V_\theta}{\partial \theta} + \frac{\partial V_z}{\partial z} = 0 , \qquad (2.3)$$

and momentum (Navier-Stokes equations):

$$\left(\frac{\partial V_r}{\partial t} + V_r \frac{\partial V_r}{\partial r} + \frac{V_\theta}{r}\frac{\partial V_r}{\partial \theta} - \frac{V_\theta^2}{r} + V_z \frac{\partial V_r}{\partial z} \right) + \frac{1}{\rho}\frac{\partial P}{\partial r}$$

$$= \nu \left(\frac{\partial^2 V_r}{\partial r^2} + \frac{1}{r}\frac{\partial V_r}{\partial r} - \frac{V_r}{r^2} + \frac{1}{r^2}\frac{\partial^2 V_r}{\partial \theta^2} - \frac{2}{r^2}\frac{\partial V_\theta}{\partial \theta} + \frac{\partial^2 V_r}{\partial z^2} \right), \qquad (2.4)$$

$$\left(\frac{\partial V_\theta}{\partial t} + V_r \frac{\partial V_\theta}{\partial r} + \frac{V_\theta}{r}\frac{\partial V_\theta}{\partial \theta} + \frac{V_r V_\theta}{r} + V_z \frac{\partial V_\theta}{\partial z} \right) + \frac{1}{\rho r}\frac{\partial P}{\partial \theta}$$

$$= \nu \left(\frac{\partial^2 V_\theta}{\partial r^2} + \frac{1}{r}\frac{\partial V_\theta}{\partial r} - \frac{V_\theta}{r^2} + \frac{1}{r^2}\frac{\partial^2 V_\theta}{\partial \theta^2} + \frac{2}{r^2}\frac{\partial V_r}{\partial \theta} + \frac{\partial^2 V_\theta}{\partial z^2} \right), \qquad (2.5)$$

and

$$\left(\frac{\partial V_z}{\partial t} + V_r \frac{\partial V_z}{\partial r} + \frac{V_\theta}{r}\frac{\partial V_z}{\partial \theta} + V_z \frac{\partial V_z}{\partial z} \right) + \frac{1}{\rho}\frac{\partial P}{\partial z}$$

$$= \nu \left(\frac{\partial^2 V_z}{\partial r^2} + \frac{1}{r}\frac{\partial V_z}{\partial r} + \frac{1}{r^2}\frac{\partial^2 V_z}{\partial \theta^2} + \frac{\partial^2 V_z}{\partial z^2} \right) , \qquad (2.6)$$

where ρ is the density and ν is the kinematic viscosity of the fluid.

The steady basic flow itself satisfies the equations

$$\left.\begin{aligned} &\frac{\partial \bar{P}^*}{\partial r} = \frac{\partial \bar{P}^*}{\partial \theta} = 0 \; ; \qquad \therefore \bar{P}^* (r, \theta, z) = \bar{P}^* (z), \\ &\text{and} \\ &\frac{1}{\rho} \frac{\partial \bar{P}^*}{\partial z} = \nu \left(\frac{\partial^2 \bar{V}_z^*}{\partial r^2} + \frac{1}{r} \frac{\partial \bar{V}_z^*}{\partial r} \right) , \end{aligned}\right\} \quad (2.7)$$

so that the basic flow has the well-known form

$$\left.\begin{aligned} &\frac{\bar{V}_z^*}{V_{av}} = \frac{2\left[(r_2^2 - r^2) \ln \frac{r_2}{r_1} + (r_2^2 - r_1^2) \ln \frac{r}{r_2}\right]}{\left[(r_2^2 + r_1^2) \ln \frac{r_2}{r_1} - (r_2^2 - r_1^2)\right]} \\ &\bar{V}_r^* = \bar{V}_\theta^* = 0 , \end{aligned}\right\} \quad (2.8)$$

where V_{av} is the average, over the flow cross-section, of the axial velocity $\bar{V}_z^*$, and r_1 and r_2 are the inner and outer radii of the annulus respectively.

If we now substitute equations (2.1) and (2.2) into equations (2.3) through (2.6), make use of equation (2.7), and neglect the product terms of disturbance velocities with themselves and with their spatial derivatives, we obtain the following set of linearized hydrodynamic equations for disturbance velocity and pressure

$$\frac{\partial v_r^*}{\partial r} + \frac{v_r^*}{r} + \frac{1}{r} \frac{\partial v_\theta^*}{\partial \theta} + \frac{\partial v_z^*}{\partial z} = 0, \quad (2.9)$$

$$\frac{\partial v_r^*}{\partial t} + \bar{V}_z^* \frac{\partial v_r^*}{\partial z} + \frac{1}{\rho} \frac{\partial p^*}{\partial r}$$

$$= \nu \left(\frac{\partial^2 v_r^*}{\partial r^2} + \frac{1}{r} \frac{\partial v_r^*}{\partial r} - \frac{v_r^*}{r^2} + \frac{1}{r^2} \frac{\partial^2 v_r^*}{\partial \theta^2} - \frac{2}{r^2} \frac{\partial v_\theta^*}{\partial \theta} + \frac{\partial^2 v_r^*}{\partial z^2} \right), \quad (2.10)$$

$$\frac{\partial v_\theta^*}{\partial t} + \bar{V}_z^* \frac{\partial v_\theta^*}{\partial z} + \frac{1}{\rho r}\frac{\partial p^*}{\partial \theta}$$

$$= \nu \left(\frac{\partial^2 v_\theta^*}{\partial r^2} + \frac{1}{r}\frac{\partial v_\theta^*}{\partial r} - \frac{v_\theta^*}{r^2} + \frac{1}{r^2}\frac{\partial^2 v_\theta^*}{\partial \theta^2} + \frac{2}{r^2}\frac{\partial v_r^*}{\partial \theta} + \frac{\partial^2 v_\theta^*}{\partial z^2} \right), \tag{2.11}$$

and

$$\frac{\partial v_z^*}{\partial t} + v_r^* \frac{\partial \bar{V}_z^*}{\partial r} + \bar{V}_z^* \frac{\partial v_z^*}{\partial z} + \frac{1}{\rho}\frac{\partial p^*}{\partial z}$$

$$= \nu \left(\frac{\partial^2 v_z^*}{\partial r^2} + \frac{1}{r}\frac{\partial v_z^*}{\partial r} + \frac{1}{r^2}\frac{\partial^2 v_z^*}{\partial \theta^2} + \frac{\partial^2 v_z^*}{\partial z^2} \right). \tag{2.12}$$

Equations (2.9) through (2.12) can be made non-dimensional by choosing as the respective units of length, velocity and density the parameters r_2, V_{av} and ρ. Thus let

$$\left.\begin{aligned} v_r &= \frac{v_r^*}{V_{av}}, \quad r' = \frac{r}{r_2}, \quad \bar{V}_z = \frac{\bar{V}_z^*}{V_{av}}, \\ v_\theta &= \frac{v_\theta^*}{V_{av}}, \quad z' = \frac{z}{r_2}, \quad p = \frac{p^*}{\rho V_{av}^2}, \\ v_z &= \frac{v_z^*}{V_{av}}, \quad t' = \frac{t\, V_{av}}{r_2}, \quad R = \frac{V_{av}\, r_2}{\nu}. \end{aligned}\right\} \tag{2.13}$$

The modified Reynolds number R is related to the actual Reynolds number R_a ($= 2 V_{av} (r_2 - r_1)/\nu$) by $R_a = 2R(1 - \gamma)$, where $\gamma = r_1/r_2$. The dimensionless basic flow velocity $\bar{V}_z$ (from equation 2.8) is given by

$$\left.\begin{aligned} \bar{V}_z &= \beta\,(1 - r^2) - \alpha \ln r \ , \\ \text{where } \alpha &= 2\,(1 - \gamma^2) \,/\, \left[(1 + \gamma^2) \ln \gamma + (1 - \gamma^2)\right], \\ \text{and } \beta &= 2 \ln \gamma \,/\, \left[(1 + \gamma^2) \ln \gamma + (1 - \gamma^2)\right] . \end{aligned}\right\} \quad (2.14)$$

Making substitutions from equations (2.13) and (2.14) into equations (2.9) through (2.12), dividing equation (2.9) by (V_{av}/r_2) and equations (2.10) through (2.12) by (V_{av}^2/r_2), and dropping the primes from r, z and t for convenience, we get the following set of linear, partial differential equations for the fluctuation properties in non-dimensional form

$$\frac{\partial v_r}{\partial r} + \frac{v_r}{r} + \frac{1}{r}\frac{\partial v_\theta}{\partial \theta} + \frac{\partial v_z}{\partial z} = 0 \ , \quad (2.15)$$

$$\frac{\partial v_r}{\partial t} + \bar{V}_z \frac{\partial v_r}{\partial z} + \frac{\partial p}{\partial r}$$

$$= \frac{1}{R}\left(\frac{\partial^2 v_r}{\partial r^2} + \frac{1}{r}\frac{\partial v_r}{\partial r} - \frac{v_r}{r^2} + \frac{1}{r^2}\frac{\partial^2 v_r}{\partial \theta^2} - \frac{2}{r^2}\frac{\partial v_\theta}{\partial \theta} + \frac{\partial^2 v_r}{\partial z^2}\right), \quad (2.16)$$

$$\frac{\partial v_\theta}{\partial t} + \bar{V}_z \frac{\partial v_\theta}{\partial z} + \frac{1}{r}\frac{\partial p}{\partial \theta}$$

$$= \frac{1}{R}\left(\frac{\partial^2 v_\theta}{\partial r^2} + \frac{1}{r}\frac{\partial v_\theta}{\partial r} - \frac{v_\theta}{r^2} + \frac{1}{r^2}\frac{\partial^2 v_\theta}{\partial \theta^2} + \frac{2}{r^2}\frac{\partial v_r}{\partial \theta} + \frac{\partial^2 v_\theta}{\partial z^2}\right), \quad (2.17)$$

and

$$\frac{\partial v_z}{\partial t} + v_r \frac{\partial \bar{V}_z}{\partial r} + \bar{V}_z \frac{\partial v_z}{\partial z} + \frac{\partial p}{\partial z}$$

$$= \frac{1}{R}\left(\frac{\partial^2 v_z}{\partial r^2} + \frac{1}{r}\frac{\partial v_z}{\partial r} + \frac{1}{r^2}\frac{\partial^2 v_z}{\partial \theta^2} + \frac{\partial^2 v_z}{\partial z^2}\right) . \quad (2.18)$$

Since the equations (2.15) through (2.18) are linear, the various Fourier components forming the arbitrary disturbance according to equation (1.4) or (1.7) are independent of one another. We can, therefore, consider only one Fourier component at a time. Thus we hope to find solutions of the type

$$\phi(r, \theta, z, t) = \mathrm{Re}\left[\hat{\phi}(r, \theta, z, t)\right]$$

$$= \mathrm{Re}\left[\bar{\phi}(r) \exp(kz + in\theta - i\omega t)\right]. \qquad (2.19)$$

Equation (2.19) is equivalent to four equations by replacing ϕ by v_r, v_θ, v_z and p successively. All variables in the equation are dimensionless, and the superscript ($\hat{}$) indicates a preliminary complex solution which will lead to the real solution ϕ. The quantity $\bar{\phi}(r)$ is a complex function of r alone. Substituting the disturbance pressure and velocity components in the form of equation (2.19) into equations (2.15) through (2.18) and eliminating the exponential factor, we get, after some rearrangement, the following set of linear, homogeneous, ordinary differential equations

$$\left(D + \frac{1}{r}\right)\bar{v}_r + \frac{n}{r}(i\bar{v}_\theta) + k\bar{v}_z = 0 , \qquad (2.20)$$

$$\left[D^2 + \frac{1}{r}D - \left\{\frac{n^2+1}{r^2} - k^2 + R(k\bar{V}_z - i\omega)\right\}\right]\bar{v}_r$$

$$- \frac{2n}{r^2}(i\bar{v}_\theta) - RD\bar{p} = 0 , \qquad (2.21)$$

$$\left[D^2 + \frac{1}{r} D - \left\{ \frac{n^2 + 1}{r^2} - k^2 + R\,(k\bar{V}_z - i\omega) \right\} \right] (i\bar{v}_\theta)$$

$$- \frac{2n}{r^2} \bar{v}_r + \frac{n}{r} R\bar{p} = 0 , \qquad (2.22)$$

and

$$\left[D^2 + \frac{1}{r} D - \left\{ \frac{n^2}{r^2} - k^2 + R\,(k\bar{V}_z - i\omega) \right\} \right] \bar{v}_z$$

$$- R\bar{v}_r D\bar{V}_z - Rk\bar{p} = 0 , \qquad (2.23)$$

where D is the operator d/dr.

For any type of stability analysis the solution of the above set yields the amplitude functions $\bar{v}_r$ (r), $\bar{v}_\theta$ (r), $\bar{v}_z$ (r) and $\bar{p}$ (r) given the value of parameters n and R. While considering the temporal stability, an imaginary value of k is assumed to find the complex ω while in the case of spatial stability, a real value of ω is assumed to find the complex k. This is done by applying the boundary conditions at the inner and outer walls of the annulus to the solutions of the differential equations (2.20) through (2.23). It may be pointed out that the dimensional counterparts of ω and k are

$$\omega^* = \frac{V_{av}\,\omega}{r_2} , \quad \text{and} \quad k^* = \frac{k}{r_2} . \qquad (2.24)$$

2.2 Boundary Conditions

The physical restrictions at the rigid, impermeable inner ($r = \gamma$) and outer ($r = 1$) walls are

$$\bar{v}_r(\gamma) = \bar{v}_\theta(\gamma) = \bar{v}_z(\gamma) = 0,\ \bar{p}(\gamma) \text{ finite}, \tag{2.25}$$

and

$$\bar{v}_r(1) = \bar{v}_\theta(1) = \bar{v}_z(1) = 0,\ \bar{p}(1) \text{ finite}. \tag{2.26}$$

For given values of real ω (for spatial stability) or imaginary k (for temporal stability) and parameters R and n, the solution of equations (2.20) through (2.23) together with the boundary conditions in equations (2.25) and (2.26) leads to an eigenvalue problem.

CHAPTER 3

SOLUTION OF STABILITY EQUATIONS

Equations (2.20) through (2.23) together with the boundary conditions in equations (2.25) and (2.26) completely govern the propagation of an arbitrary, infinitesimal disturbance through an incompressible, viscous, coaxial annular flow. Their solution will determine whether such a disturbance grows or decays with the downstream distance z (for spatial analysis) or with time t (for temporal analysis). In terms of k or ω, the flow would be spatially unstable when $k_r > 0$ and temporally unstable when $\omega_i > 0$, where k_r and ω_i are the real and imaginary parts of k and ω respectively.

The set of differential equations (2.20) through (2.23) are too complex to be amenable to an analytical solution and, therefore, numerical technique has been used for the solution. Direct integration of these differential equations by means of, say the Runge-Kutta method, is not possible since all the starting values for the eigenfunctions and their derivatives are not known. In order to get these starting values, the eigenfunctions are expanded as a power series in (1 - r) near the outer wall for small (1 - r). The preference of (1 - r) over r for the series solution is based on the form of the basic flow velocity $\bar{V}_z$, which being in terms of ln r, can be expanded easily in terms of (1 - r), as

$$\bar{V}_z(r) = C_1(1-r) + C_2(1-r)^2 + \ldots + C_m(1-r)^m + \ldots, \quad (3.1)$$

where $C_1 = \alpha + 2\beta$, $C_2 = (\alpha/2) - \beta$,

$C_m = \alpha/m$; $m = 3, 4, \ldots$.

The expressions $1/r$ and $1/r^2$ in equations (2.20) through (2.23) are written as

$$\left.\begin{aligned} \frac{1}{r} = \frac{1}{1-(1-r)} &= 1 + (1-r) + (1-r)^2 + \ldots + (1-r)^m \\ &\quad + \ldots , \\ \text{and} \\ \frac{1}{r^2} = \frac{1}{[1-(1-r)]^2} &= 1 + 2(1-r) + 3(1-r)^2 + \ldots \\ &\quad + m(1-r)^{m-1} + \ldots \end{aligned}\right\} \quad (3.2)$$

respectively. Starting from the outer wall $[(1-r) = 0]$, the series solution is carried up to a small but finite value of $(1-r)$ (for example $(1-r) = 0.05$ i.e. $r = 0.95$) due to practical difficulties of summing a very large number of terms. The solution is then continued by the fourth order Runge-Kutta method to the inner wall ($r = \gamma$). The whole procedure is iterated until the boundary conditions at the inner wall are satisfied, thus resulting in a value for the eigenvalue k (for spatial stability) or eigenvalue ω (for temporal stability).

3.1 Series Expansion

Let the power series expansion of $\bar{v}_r$, $i\bar{v}_\theta$, $\bar{v}_z$ and $\bar{p}$ be of the form

$$\bar{v}_r = (1-r)^a \left[V_1 + V_2(1-r) + V_3(1-r)^2 + \ldots + V_m(1-r)^{m-1} + \ldots\right], \quad (3.3)$$

$$i\bar{v}_\theta = (1-r)^b \left[W_1 + W_2(1-r) + W_3(1-r)^2 + \ldots + W_m(1-r)^{m-1} + \ldots\right], \quad (3.4)$$

$$\bar{v}_z = (1-r)^c \left[U_1 + U_2 (1-r) + U_3 (1-r)^2 + \ldots + U_m (1-r)^{m-1} + \ldots \right], \tag{3.5}$$

and

$$\bar{p} = (1-r)^d \left[P_1 + P_2 (1-r) + P_3 (1-r)^2 + \ldots + P_m (1-r)^{m-1} + \ldots \right], \tag{3.6}$$

where all V, W, U and P's are complex constants.

Substituting equations (3.1) through (3.6) into differential equations (2.20) through (2.23), we get from equation (2.20)

$$\begin{aligned}
&- (1-r)^{a-1} aV_1 + (1-r)^a \left[V_1 - (a+1) V_2 \right] + (1-r)^{a+1} \left[V_1 + V_2 \right. \\
&\left. - (a+2) V_3 \right] + \ldots + (1-r)^{a+m-2} \left[\left\{ \sum_{j=1}^{m-1} V_j \right\} - (a+m-1) V_m \right] + \ldots \\
&+ (1-r)^b nW_1 + (1-r)^{b+1} n (W_1+W_2) + \ldots \\
&+ (1-r)^{b+m-2} \left[n \left\{ \sum_{j=1}^{m-1} W_j \right\} \right] + \ldots + (1-r)^c kU_1 \\
&+ (1-r)^{c+1} kU_2 + \ldots + (1-r)^{c+m-2} kU_{m-1} + \ldots = 0,
\end{aligned} \tag{3.7}$$

from equation (2.21)

$$\begin{aligned}
&(1-r)^{a-2} \left[(a-1) aV_1 \right] + (1-r)^{a-1} \left[a(a+1) V_2 - aV_1 \right] \\
&+ (1-r)^a \left[(a+1)(a+2) V_3 - aV_1 - (a+1) V_2 - (n^2+1) V_1 \right. \\
&\left. + (k^2+i\omega R) V_1 \right] + (1-r)^{a+1} \left[(a+2)(a+3) V_4 - aV_1 \right. \\
&-(a+1) V_2 - (a+2) V_3 - (n^2+1) (V_2+2V_1) - RkC_1 V_1 \\
&\left. + (k^2+i\omega R) V_2 \right] + \ldots + (1-r)^{a+m-3} \left[(a+m-2)(a+m-1) V_m \right.
\end{aligned}$$

$$-\left\{\sum_{j=1}^{m-1}(a+j-1)\,V_j\right\}-(n^2+1)\left\{\sum_{j=1}^{m-2}(m-j-1)\,V_j\right\}$$

$$-Rk\left\{\sum_{j=1}^{m-3}C_j\,V_{m-j-2}\right\}+(k^2+i\omega R)\,V_{m-2}\Big]+\ldots$$

$$-(1-r)^b\,2nW_1-(1-r)^{b+1}\,2n\,(2W_1+W_2)-\ldots$$

$$-(1-r)^{b+m-1}\,2n\left[\sum_{j=1}^{m}(m-j+1)\,W_j\right]\quad-\ldots$$

$$+(1-r)^{d-1}\,RdP_1+(1-r)^d\,R\,(d+1)\,P_2+\ldots$$

$$+(1-r)^{d+m-2}\,R\,(d+m-1)\,P_m+\ldots=0\,, \qquad (3.8)$$

from equation (2.22)

$$(1-r)^{b-2}\left[(b-1)\,bW_1\right]+(1-r)^{b-1}\left[b(b+1)\,W_2-bW_1\right]$$

$$+(1-r)^b\left[(b+1)(b+2)\,W_3-bW_1-(b+1)\,W_2-(n^2+1)\,W_1\right.$$

$$\left.+(k^2+i\omega R)\,W_1\right]+(1-r)^{b+1}\left[(b+2)(b+3)\,W_4-bW_1-(b+1)\,W_2\right.$$

$$\left.-(b+2)\,W_3-(n^2+1)(W_2+2W_1)-RkC_1W_1+(k^2+i\omega R)\,W_2\right]+\ldots$$

$$+(1-r)^{b+m-3}\left[(b+m-2)(b+m-1)W_m-\left\{\sum_{j=1}^{m-1}(b+j-1)\,W_j\right\}\right.$$

$$-(n^2+1)\left\{\sum_{j=1}^{m-2}(m-j-1)\,W_j\right\}-Rk\left\{\sum_{j=1}^{m-3}C_j\,W_{m-j-2}\right\}$$

$$\left.+(k^2+i\omega R)\,W_{m-2}\right]+\ldots-(1-r)^a\,2nV_1-(1-r)^{a+1}$$

$$2n\,(2V_1+V_2)-\ldots-(1-r)^{a+m-1}\,2n\left\{\sum_{j=1}^{m}(m-j+1)\,V_j\right\}-\ldots$$

$$+(1-r)^d\,nRP_1+(1-r)^{d+1}\,nR\,(P_1+P_2)+\ldots$$

$$+(1-r)^{d+m-1}\,nR\left(\sum_{j=1}^{m}P_j\right)+\ldots=0\,, \qquad (3.9)$$

and from equation (2.23)

$$(1-r)^{c-2}\left[(c-1)\ cU_1\right] + (1-r)^{c-1}\left[c(c+1)\ U_2 - cU_1\right]$$
$$+ (1-r)^{c}\left[(c+1)(c+2)\ U_3 - cU_1 - (c+1)\ U_2 - n^2U_1\right.$$
$$\left. + (k^2+i\omega R)\ U_1\right] + (1-r)^{c+1}\left[(c+2)(c+3)\ U_4 - cU_1 - (c+1)\ U_2\right.$$
$$\left. - (c+2)\ U_3 - n^2\ (U_2 + 2U_1) - RkC_1U_1 + (k^2+i\omega R)\ U_2\right] + \ldots$$
$$+ (1-r)^{c+m-3}\left[(c+m-2)(c+m-1)\ U_m - \left\{\sum_{j=1}^{m-1} (c+j-1)\ U_j\right\}\right.$$
$$- n^2\left\{\sum_{j=1}^{m-2} (m-j-1)\ U_j\right\} - Rk\left\{\sum_{j=1}^{m-3} C_j\ U_{m-j-2}\right\}$$
$$\left. + (k^2+i\omega R)\ U_{m-2}\right] + \ldots + (1-r)^{a}\ RC_1V_1 + (1-r)^{a+1}$$
$$R\ (2C_2V_1 + C_1V_2) + \ldots + (1-r)^{a+m-1}\ R\left\{\sum_{j=1}^{m} jC_j\ V_{m-j+1}\right\} + \ldots$$
$$- (1-r)^{d}\ RkP_1 - (1-r)^{d+1}\ RkP_2 - (1-r)^{d+2}\ RkP_3 - \ldots$$
$$- (1-r)^{d+m-1}\ RkP_m - \ldots = 0. \qquad (3.10)$$

In equations (3.7) through (3.10) any term with either a zero or negative subscript is set to zero.

To find relations for a, b, c and d, the coefficient of r^s is set to zero for all s in equations (3.7) through (3.10). This gives

A From equation (3.7)

either one or more of the three factors (a-1), b and c is the smallest.

(i) If (a-1) is the smallest,

$aV_1 = 0$ i.e. either $a = 0$ or $V_1 = 0$.

(ii) If b is the smallest,

$nW_1 = 0$ i.e. $W_1 = 0$ for $n \neq 0$.

(iii) If c is the smallest,

$kU_1 = 0$ i.e. $U_1 = 0$ ($\because k \neq 0$).

(iv) If all or any two of these three factors are equal but V_1, W_1 and U_1 are independent, we get precisely the same conclusions as above; in case the corresponding V_1, W_1 and U_1 are dependent, no useful relation can be found for a, b and c.

B From equation (3.8)

either one or more of the three factors (a-2), b and (d-1) is the smallest.

(i) If (a-2) is the smallest,

$(a-1)\, aV_1 = 0$ i.e. either $a = 0$ or 1 or $V_1 = 0$.

(ii) If b is the smallest,

$2\, nW_1 = 0$ i.e. $W_1 = 0$ for $n \neq 0$.

(iii) If (d-1) is the smallest,

$RdP_1 = 0$ i.e. either $d = 0$ or $P_1 = 0$ ($\because R \neq 0$)

(iv) Remarks similar to those in A (iv) hold if two or all of these three factors are equal.

C From equation (3.9)

either one or more of the three factors (b-2), a and d is the smallest.

(i) If (b-2) is the smallest,

$(b-1)\, bW_1 = 0$ i.e. either $b = 0$ or 1 or $W_1 = 0$.

(ii) If a is the smallest,

$2\, nV_1 = 0$ i.e. $V_1 = 0$ for $n \neq 0$.

(iii) If d is the smallest,

$nRP_1 = 0$ i.e. $P_1 = 0$ for $n \neq 0$.

(iv) Remarks similar to those in A (iv) hold if two or all of these three factors are equal.

D From equation (3.10)

either one or more of the three factors (c-2), a and d is the smallest.

(i) If (c-2) is the smallest,

$(c-1)\, cU_1 = 0$ i.e. either $c = 0$ or 1 or $U_1 = 0$.

(ii) If a is the smallest

$RC_1V_1 = 0$ i.e. $V_1 = 0$ ($\because C_1 \neq 0$)

(iii) If d is the smallest

$RkP_1 = 0$ i.e. $P_1 = 0$.

(iv) Remarks similar to those in A (iv) hold if two or all of these three factors are equal.

Looking over these conclusions, we take

$$a = b = c = 1,\ d = 0 \text{ and } V_1 = 0 \qquad (3.11)$$

so that the boundary conditions at r = 1 are satisfied.

The recurrence relations for the constants in the series expansions can now be determined by substituting equation (3.11) into equations (3.7) through (3.10). We arrange the terms in ascending powers of (1-r), and equate the coefficient for the $(m-1)^{th}$ term in each equation to zero to get

from equation (3.7)

$$(1-r)^{m-1} : \left\{ \sum_{j=2}^{m-1} V_j \right\} - mV_m + n \left\{ \sum_{j=1}^{m-1} W_j \right\} + kU_{m-1} = 0, \qquad (3.12)$$

from equation (3.8)

$$\begin{aligned} (1-r)^{m-2} : \quad & (m-1)\, mV_m - \left\{ \sum_{j=2}^{m-1} jV_j \right\} - (n^2+1) \left\{ \sum_{j=2}^{m-2} (m-j-1)\, V_j \right\} \\ & - Rk \left\{ \sum_{j=1}^{m-4} C_j\, V_{m-j-2} \right\} + (k^2 + i\omega R)\, V_{m-2} \\ & - 2n \left\{ \sum_{j=1}^{m-2} (m-j-1)\, W_j \right\} + R(m-1)\, P_m = 0, \qquad (3.13) \end{aligned}$$

from equation (3.9)

$$\begin{aligned} (1-r)^{m-2} : \quad & (m-1)m\, W_m - \left\{ \sum_{j=1}^{m-1} jW_j \right\} - (n^2+1) \left\{ \sum_{j=1}^{m-2} (m-j-1)\, W_j \right\} \\ & - Rk \left\{ \sum_{j=1}^{m-3} C_j\, W_{m-j-2} \right\} + (k^2+i\omega R)\, W_{m-2} \\ & - 2n \left\{ \sum_{j=2}^{m-2} (m-j-1)\, V_j \right\} + nR \left(\sum_{j=1}^{m-1} P_j \right) = 0, \qquad (3.14) \end{aligned}$$

and from equation (3.10)

$$(1-r)^{m-2} : (m-1)\, mU_m - \left\{\sum_{j=1}^{m-1} jU_j\right\} - n^2 \left\{\sum_{j=1}^{m-2} (m-j-1)\, U_j\right\}$$

$$- Rk \left\{\sum_{j=1}^{m-3} C_j\, U_{m-j-2}\right\} + (k^2+i\omega R)\, U_{m-2}$$

$$+ R \left\{\sum_{j=1}^{m-3} jC_j\, V_{m-j-1}\right\} - Rk\, P_{m-1} = 0, \qquad (3.15)$$

where again any term with either a zero or negative subscript is set to zero by convention.

The equations (3.12) through (3.15) are identically true for m =1. Since $V_1 = 0$, only U_1, P_1 and W_1 are independent. For determination of all the higher subscripted V, U, P and W's, we note that equation (3.12) gives V_m, equation (3.14) gives W_m, equation (3.15) gives U_m, and equation (3.13) after substituting for V_m from equation (3.12) gives P_m. Thus replacing m by (m+1) in equations (3.12) through (3.15), we get

$$V_{m+1} = \frac{1}{(m+1)} \left(\sum_{j=2}^{m} V_j\right) + \frac{n}{(m+1)} \left(\sum_{j=1}^{m} W_j\right) + \frac{k}{(m+1)}\, U_m, \qquad (3.16)$$

$$W_{m+1} = \frac{1}{(m+1)} \left(\sum_{j=1}^{m} W_j\right) - \frac{nR}{m(m+1)} \left(\sum_{j=1}^{m} P_j\right)$$

$$+ \frac{n^2}{m(m+1)} \left\{\sum_{j=1}^{m-1} (m-j)\, W_j\right\} - \frac{(k^2+i\omega R)}{m\,(m+1)}\, W_{m-1}$$

$$+ \frac{2n}{m(m+1)} \left\{\sum_{j=2}^{m-1} (m-j)\, V_j\right\} + \frac{kR}{m(m+1)} \left\{\sum_{j=1}^{m-2} C_j\, W_{m-j-1}\right\}, \qquad (3.17)$$

$$U_{m+1} = \frac{1}{m(m+1)} \left(\sum_{j=1}^{m} jU_j \right) + \frac{n^2}{m(m+1)} \left\{ \sum_{j=1}^{m-1} (m-j)\, U_j \right\}$$

$$- \frac{(k^2+i\omega R)}{m(m+1)}\, U_{m-1} - \frac{R}{m(m+1)} \left\{ \sum_{j=1}^{m-2} jC_j\, V_{m-j} \right\}$$

$$+ \frac{kR}{m(m+1)} \left\{ \sum_{j=1}^{m-2} C_j\, U_{m-j-1} \right\} + \frac{kR}{m(m+1)}\, P_m, \qquad (3.18)$$

and

$$P_{m+1} = - \frac{n}{R} \left(\sum_{j=1}^{m} W_j \right) - \frac{k}{R}\, U_m + \frac{n^2}{mR} \left\{ \sum_{j=2}^{m-1} (m-j)\, V_j \right\}$$

$$- \frac{(k^2+i\omega R)}{mR}\, V_{m-1} + \frac{2n}{mR} \left\{ \sum_{j=1}^{m-1} (m-j)\, W_j \right\}$$

$$+ \frac{k}{m} \left\{ \sum_{j=1}^{m-3} C_j\, V_{m-j-1} \right\}, \qquad (3.19)$$

with $V_1 = 0$. (3.20)

In that order, equations (3.16) through (3.19) give the coefficients V_m, W_m, U_m and P_m for $m = 2, 3, 4, \ldots$ in terms of U_1, P_1 and W_1. With all coefficients in the series solutions (equations (3.3) through (3.6)) expressed in terms of U_1, P_1 and W_1, we can express any eigenfunction as a sum of <u>three</u> terms; for example the radial velocity eigenfunction $\bar{v}_r(r)$ may be written as

$$\bar{v}_r(r) = v_{r1}(r)\, U_1 + v_{r2}(r)\, P_1 + v_{r3}(r)\, W_1. \qquad (3.21)$$

A similar expansion holds for the other eigenfunctions $\bar{v}_\theta(r)$, $\bar{v}_z(r)$ and $\bar{p}(r)$.

3.2 Step-by-Step Integration

Starting from the outer wall of the annulus (i.e. $r = 1$) the series expansions developed above are carried only up to a small value of $(1 - r)$. The solution is further continued by a step-by-step integration technique to the inner wall of the annulus. The equations (2.20) through (2.23) are not directly useful for the step-by-step integration technique due to the fact that equation (2.21) contains both the highest degree derivatives in the eigenfunction $\bar{v}_r(r)$ and $\bar{p}(r)$. To circumvent this difficulty, we differentiate the continuity equation (equation (2.20)) with respect to r and solve for $D^2 \bar{v}_r$. The equation (2.21) can be solved for the unknown $D\bar{p}$ using the relation just obtained for $D^2 \bar{v}_r$, and equations (2.22) and (2.23) give $D^2 (i\bar{v}_\theta)$ and $D^2 \bar{v}_z$ respectively to yield the following set

$$D^2 \bar{v}_r = \frac{1}{r}\left(\frac{1}{r} - D\right)\left\{\bar{v}_r + n\,(i\bar{v}_\theta)\right\} - k\,D\bar{v}_z\,, \qquad (3.22)$$

$$D^2 (i\bar{v}_\theta) = \frac{n}{r}\left(\frac{2}{r}\bar{v}_r - R\bar{p}\right) + \left\{\frac{n^2+1}{r^2} - \frac{D}{r} - k^2 + R\,(k\bar{V}_z - i\omega)\right\}(i\bar{v}_\theta), \qquad (3.23)$$

$$D^2 \bar{v}_z = R\,(k\bar{p} + \bar{v}_r D\bar{V}_z) + \left\{\frac{n^2}{r^2} - \frac{D}{r} - k^2 + R\,(k\bar{V}_z - i\omega)\right\}\bar{v}_z\,, \qquad (3.24)$$

and

$$D\bar{p} = \frac{1}{R}\left[(D^2 + \frac{1}{r}D)\,\bar{v}_r - \frac{2n}{r^2}(i\bar{v}_\theta) - \left\{\frac{n^2+1}{r^2} - k^2 + R(k\bar{V}_z - i\omega)\right\}\bar{v}_r\right]. \qquad (3.25)$$

The integration of these differential equations is carried out in terms of the three independent solutions of the eigenfunctions, that is, in terms of $v_{r1}(r)$, $v_{r2}(r)$ and $v_{r3}(r)$ for the eigenfunction $\bar{v}_r(r)$, and similarly for $\bar{v}_\theta(r)$, $\bar{v}_z(r)$ and $\bar{p}(r)$.

The fourth order Runge-Kutta method, used for it, is summarized in Appendix I.

3.3 Satisfying Boundary Conditions at the Inner Wall

Having integrated the stability equations over the whole region $\gamma \leq r \leq 1$ such that boundary conditions at the outer wall of the annulus are satisfied (by means of the series expansion), it is now required to satisfy the boundary conditions at the inner wall. For n = 0 the eigenfunction $\bar{v}_\theta(r)$ in the equations (2.20) through (2.23) decouples itself completely from others. Within the context of stability theory, there is, therefore, no production of $\bar{v}_\theta(r)$ and we can arbitrarily assume that it vanishes under the effect of viscosity [7 , page 229]. Thus the set of four equations (equations (2.20) through (2.23)) reduces to one of three equations only. Thus, the case of axi-symmetric disturbances differs from that of the non-axi-symmetric disturbances in the following manner:

(i) There are three eigenfunctions and, therefore, three differential equations for the axisymmetric disturbance as compared to four for the non-axisymmetric disturbance.

(ii) There are two independent solutions for each eigenfunction and two boundary conditions at the inner wall for an axisymmetric disturbance in place of three for the non-axisymmetric disturbance.

We will, therefore, consider the two cases separately for satisfying the boundary conditions at the inner wall.

3.3.1 Axisymmetric Disturbances (n = 0)

As explained above, the eigenfunctions for an axisymmetric disturbance can be expressed in terms of only two constants U_1 and P_1; for example, the axial velocity eigenfunction $\bar{v}_z(r)$ may be written as

$$\bar{v}_z(r) = v_{z1}(r)\, U_1 + v_{z2}(r)\, P_1. \qquad (3.26)$$

The boundary conditions at the inner wall require that the disturbance velocity components be zero at $r = \gamma$, so that in view of equation (3.26), we have

$$\begin{bmatrix} v_{r1}(\gamma) & v_{r2}(\gamma) \\ v_{z1}(\gamma) & v_{z2}(\gamma) \end{bmatrix} \begin{bmatrix} U_1 \\ P_1 \end{bmatrix} = \underset{\sim}{0}; \qquad (3.27)$$

If det stands for the determinant of the coefficient

matrix, it is required that det be zero for a non-trivial solution of the set of homogeneous equations (3.27). Since the determinant det is, in general, complex, we need to ensure that the absolute value of det be zero, that is,

$$\left|\det\right| = 0. \tag{3.28}$$

Further, since the elements of the determinant in equation (3.28) are functions of k, ω and R, only certain combinations of these parameters will allow this equation to be satisfied, thus yielding the eigenvalue k (for spatial analysis) or the eigenvalue ω (for temporal analysis). Once an eigenvalue is found, the eigenfunctions $\bar{v}_r(r)$, $\bar{v}_z(r)$ and $\bar{p}(r)$ are easily calculated in terms of only one arbitrary constant, say U_1, since P_1 and U_1 are now related by equation (3.27) as

$$\frac{P_1}{U_1} = -\frac{v_{r1}(Y)}{v_{r2}(Y)} = -\frac{v_{z1}(Y)}{v_{z2}(Y)}\ . \tag{3.29}$$

For convenience, we set $U_1 = (1.0 + i\ 0.0)$, and find all the eigenfunctions from equations of the form given in equation (3.26).

3.3.2 Non-axisymmetric Disturbances ($n \neq 0$)

Following an analysis similar to that above for axisymmetric disturbances, it is obvious that the boundary conditions at the inner wall will be satisfied if

$$\begin{bmatrix} v_{r1}(\gamma) & v_{r2}(\gamma) & v_{r3}(\gamma) \\ v_{\theta 1}(\gamma) & v_{\theta 2}(\gamma) & v_{\theta 3}(\gamma) \\ v_{z1}(\gamma) & v_{z2}(\gamma) & v_{z3}(\gamma) \end{bmatrix} \begin{bmatrix} U_1 \\ W_1 \\ P_1 \end{bmatrix} = \underset{\sim}{0}. \quad (3.30)$$

The determinant, whose absolute value should be zero, is, therefore, of order 3 in contrast to that of order 2 in the case of an axisymmetric disturbance. Thus, the complex eigenvalue is again found by satisfying equation (3.28) where det is now given by the following

$$\det = \begin{vmatrix} v_{r1}(\gamma) & v_{r2}(\gamma) & v_{r3}(\gamma) \\ v_{\theta 1}(\gamma) & v_{\theta 2}(\gamma) & v_{\theta 3}(\gamma) \\ v_{z1}(\gamma) & v_{z2}(\gamma) & v_{z3}(\gamma) \end{vmatrix}. \quad (3.31)$$

The ratios of W_1 and P_1 to U_1 are given by (see equation (3.30))

$$\frac{W_1}{U_1} = \frac{v_{\theta 3}(\gamma)\, v_{z1}(\gamma) - v_{\theta 1}(\gamma)\, v_{z3}(\gamma)}{v_{\theta 2}(\gamma)\, v_{z3}(\gamma) - v_{\theta 3}(\gamma)\, v_{z2}(\gamma)}, \quad (3.32)$$

and

$$\frac{P_1}{U_1} = \frac{v_{\theta 1}(\gamma)\, v_{z2}(\gamma) - v_{\theta 2}(\gamma)\, v_{z1}(\gamma)}{v_{\theta 2}(\gamma)\, v_{z3}(\gamma) - v_{\theta 3}(\gamma)\, v_{z2}(\gamma)}, \quad (3.33)$$

so that arbitrarily setting $U_1 = (1.0 + i\ 0.0)$, the eigenfunctions can be found from equations of the form given in equation (3.21).

CHAPTER 4

RESULTS AND DISCUSSION

The disturbance equations were solved on an IBM 7044 Computer using double precision mode. The computer programme, included in Appendix III, can be used for studying both the spatial and temporal stability of flow in a concentric annulus to infinitesimal axisymmetric and non-axisymmetric disturbances. However, results are presented here only for the spatial stability of annular flow to axisymmetric disturbances. The dimensionless frequency ω was given three different values 0.1, 0.5 and 1.0 while the modified Reynolds number R was varied from 1,000 to 10,000. Three different annuli were considered with diameter ratio γ = 0.2, 0.5 and 0.8.

4.1 Computational Procedure

It is an unfortunate fact that the values of the constants (V, U and P's in equations (3.16), (3.18) and (3.19)) increase as more terms are retained in the series expansions of the eigenfunctions. Fortunately, however, the exponent of (1-r) also increases rapidly and since a term in the series consists of the product like $V_m (1-r)^{2(m-1)}$, it was found that for (1-r) less than 1, the successive terms in the series decrease in magnitude. Then if r_s represents the preassigned value

of r up to which the series solution was carried starting from the outer wall, the criteria used for terminating the series was that for $r = r_s$, the ratio of the last term retained to the partial sum up to a term preceding the last one must be less than a preassigned epsilon. This ratio was found for all the three series (equations (3.16), (3.18) and (3.19))and the maximum of these ratios was required to be less than epsilon. In view of the accuracy requirements, a value of 10^{-10} was used for epsilon in all cases. It was found that the number of terms required in the series varied from 9 to 25 for a typical r_s of 0.9; the higher number of terms required for a larger value of the parameter R. The values of the basic flow velocity and its derivative as calculated by the series (equation (3.1)) and by the actual formula (equation (2.14)) were compared and found to be the same up to at least seven significant figures even if only five terms were retained in series. The step size used for the fourth order Runge-Kutta method was taken as 0.005.

It is a well known fact [8, 9] that the error involved in the Runge-Kutta method is not easily traceable. Collatz [8, page 71] has provided a rough guide for finding a reasonable length of the integration step but in application to this problem, it was found that

his criteria was too stiff to be practicable. Ralston [9] has provided some error estimates for the Runge-Kutta method but they are good only for a single differential equation while we have three coupled differential equations for an axisymmetric disturbance. It may be noted, however, that up to R = 10,000, no numerical instability was encountered in any of the cases studied.

4.2 Stability

Since the flow is spatially unstable if the real part of the complex wave number k is greater than zero, regions in the first quadrant of the complex k-plane were explored for any possible eigenvalues by the search technique described in Appendix II. Some of the regions examined are shown in figure 4.1. No eigenvalue was found to exist inside these regions concluding, thereby, that for an infinitesimal disturbance propagating downstream all the eigenvalues for $R \leqslant 10,000$ had negative real parts. Thus, the flow in a concentric annulus was found to be spatially stable to infinitesimal axisymmetric disturbances up to a modified Reynolds number of 10,000. These results are in agreement with those of Mott and Joseph for temporal stability [6].

4.3 The Least Stable Mode

It may be recalled that for a linear stability analysis, every component of the double Fourier series forming the arbitrary disturbance (cf. equation (1.7)) can be considered independently. Thus, even though there are an infinite number of modes governing the propagation of the disturbance, the most predominant one is the least stable mode (one for which $|k_r|$ is minimum) or an unstable mode (if one exists). Results are, therefore, presented here (in figures 4.2 through 4.10) for the least stable mode since no unstable mode was found for annular flow up to R = 10,000.

Figures 4.2 through 4.4 show the variation of k_r with R (or R_a) for the least stable mode with ω as a parameter. Each figure corresponds to a different diameter ratio γ. For a particular γ, it is seen that each k_r - R curve has two branches. Below a certain Reynolds number k_r for the least stable mode follows one curve and above this Reynolds number, it follows another curve. The Reynolds number, at which such a change of branch occurs, is itself a function of ω. As ω is increased, this Reynolds number shifts to a lower value. This behaviour is found for all the three diameter ratios except for a slight abnormality for $\gamma = 0.5$. It is also to be noted that for a fixed frequency and diameter

ratio, the least stable mode becomes less stable (since $|k_r|$ decreases) as the Reynolds number increases. This suggests a possibility of there being a critical Reynolds number above which the flow may be unstable. Figures 4.2 through 4.4 indicate, however, that even if it exists, the critical Reynolds number would be much larger than 10,000 - the maximum value of R considered here. These figures also show that the annular flow is more stable to a higher frequency disturbance for a fixed Reynolds number and diameter ratio; the effect (of ω on k_r) becoming less predominant as the diameter ratio increases. Also, the effect of increasing the diameter ratio of the annulus is to make the flow more stable for a given ω and R. Mott and Joseph [6] also found a similar behaviour in the case of temporal stability.

The variation of k_i with R (or R_a) for the least stable mode is shown in figures 4.5 through 4.7 with ω as a parameter; each figure corresponding to a different diameter ratio γ. These figures are quite similar to those discussed above. Here also, for each ω and γ, the k_i - R curve is found to have two branches. However, for a fixed frequency and diameter ratio the wavelength ($= 1/k_i$) remains almost constant as R increases ten fold while $|k_r|$ decreases by a factor of about four for the same rise in R. The dimensionless phase velocity

C_p ($=\omega/k_i$) of the least stable mode is nearly unity (see tables 4-1 through 4-3). It may be observed that for a particular ω and γ, C_p increases with R and tends to a nearly constant value. This increase is maximum around the Reynolds number where a break in the k_i - R curves occurs. Moreover, for a fixed Reynolds number, the phase velocity increases with ω (γ held constant) and also with γ (ω held constant).

Figures 4.8 through 4.10 show the variation of k_r R with ωR for different diameter ratios. These curves were plotted to see whether, as in the case of pipe Poiseuille flow [4], any simple relation exists between kR and ωR. If such a relation does exist, ωR would be the governing parameter rather than the frequency ω and the modified Reynolds number R independently. Figures 4.8 through 4.10, however, indicate that, contrary to that for flow in a pipe, ωR cannot be taken as the governing parameter for flow in a concentric annulus. These figures show that as the diameter ratio increases the number of branches of the k_rR - ωR curve decreases.

Some results are also tabulated in tables 4-1 through 4-3. These tables display a few modes that are more stable than the corresponding least stable mode. Though some of these more stable modes are very close to

the corresponding least stable mode (cf. S.Nos. 9 and 12 table 4-1, S.Nos. 3 and 16 table 4-2, and S.Nos. 9 and 14 table 4-3), the eigenvalue search technique coupled with the iterative scheme was able to isolate them without much difficulty.

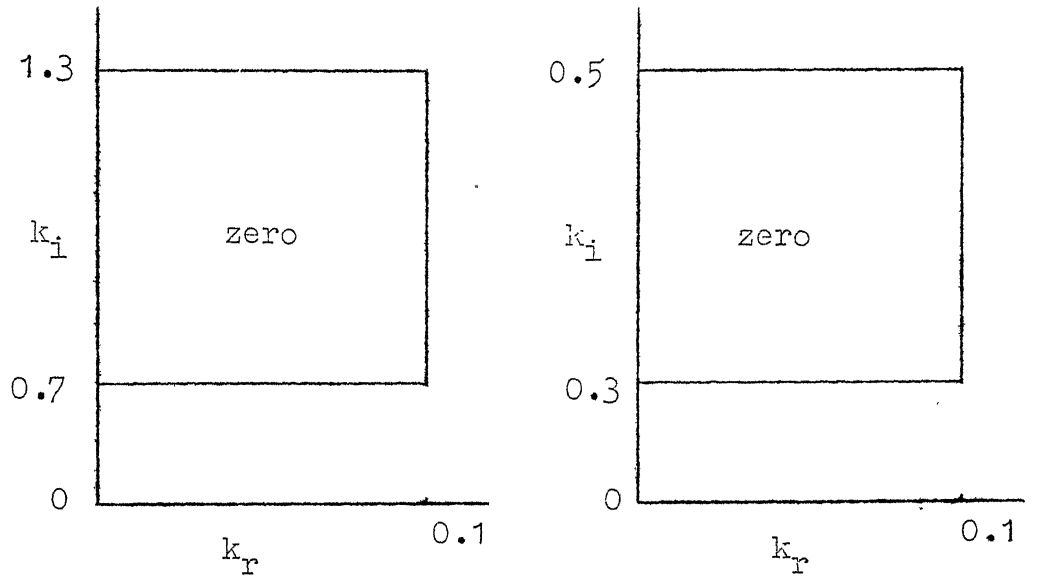

a) $\gamma = 0.2$
R = 10,000
$\omega = 1.0$

b) $\gamma = 0.2$
R = 10,000
$\omega = 0.5$

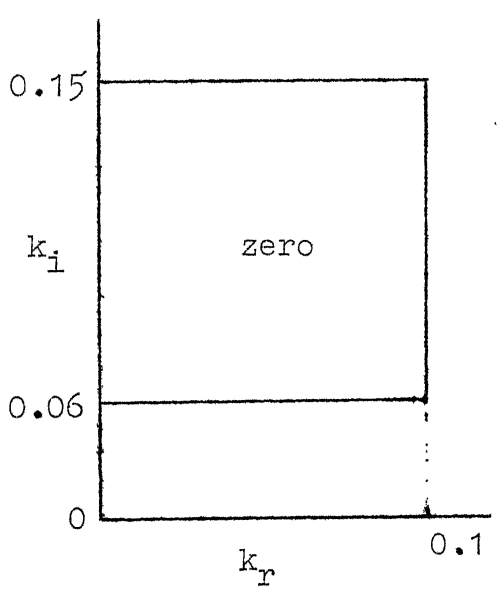

c) $\gamma = 0.5$
R = 8,000
$\omega = 0.1$

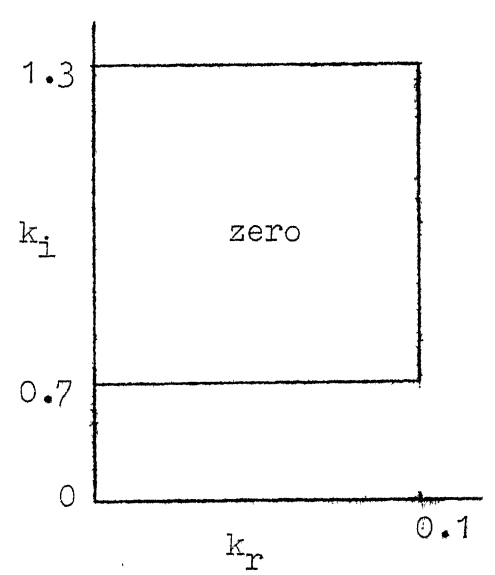

d) $\gamma = 0.8$
R = 10,000
$\omega = 1.0$

Figure 4.1 Regions on the complex k-plane with the number of eigenvalues present inside the region.

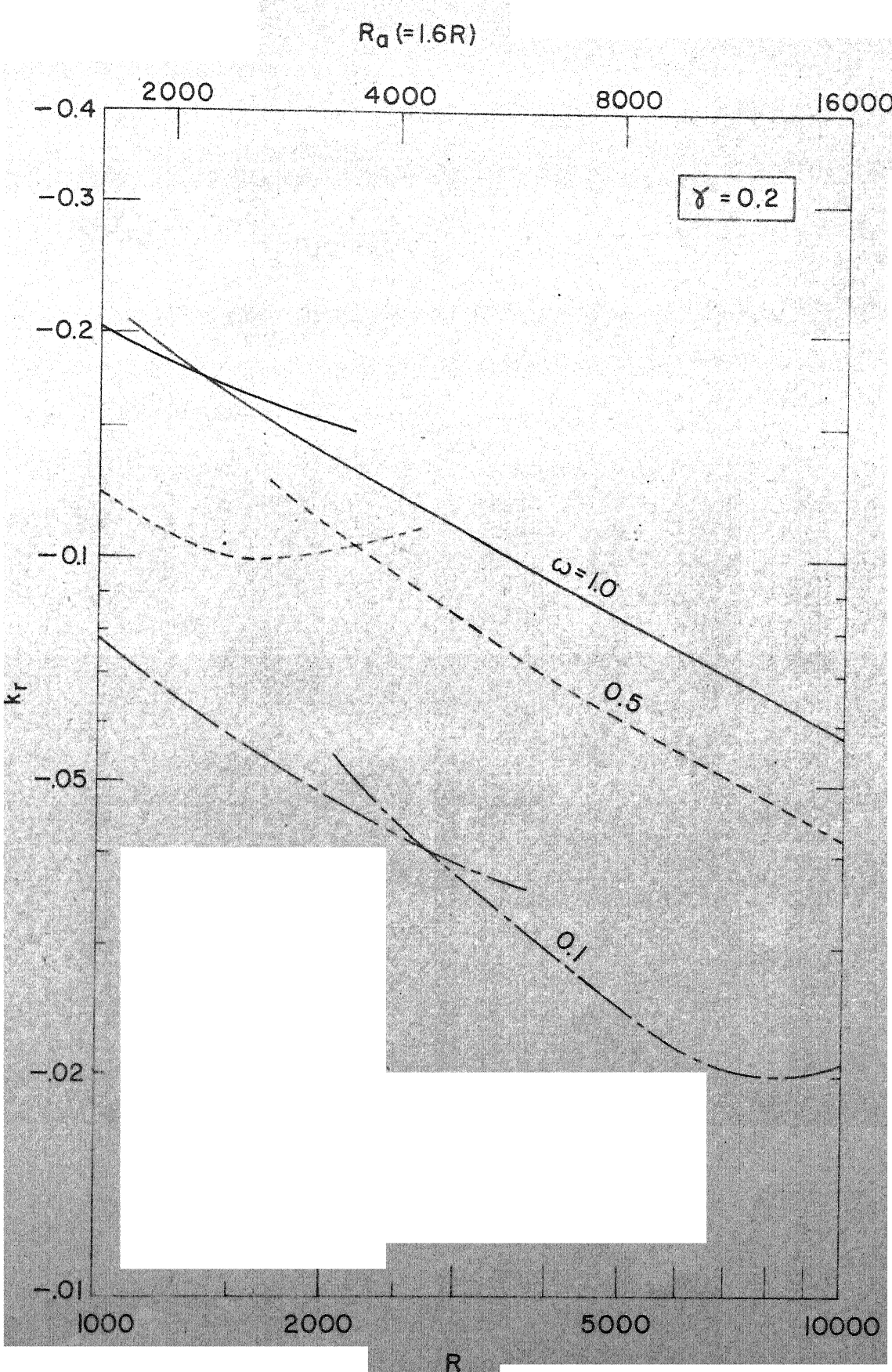

Figure 4.2 Variation of k_r with R for the Least Stable Mode for Different ω.

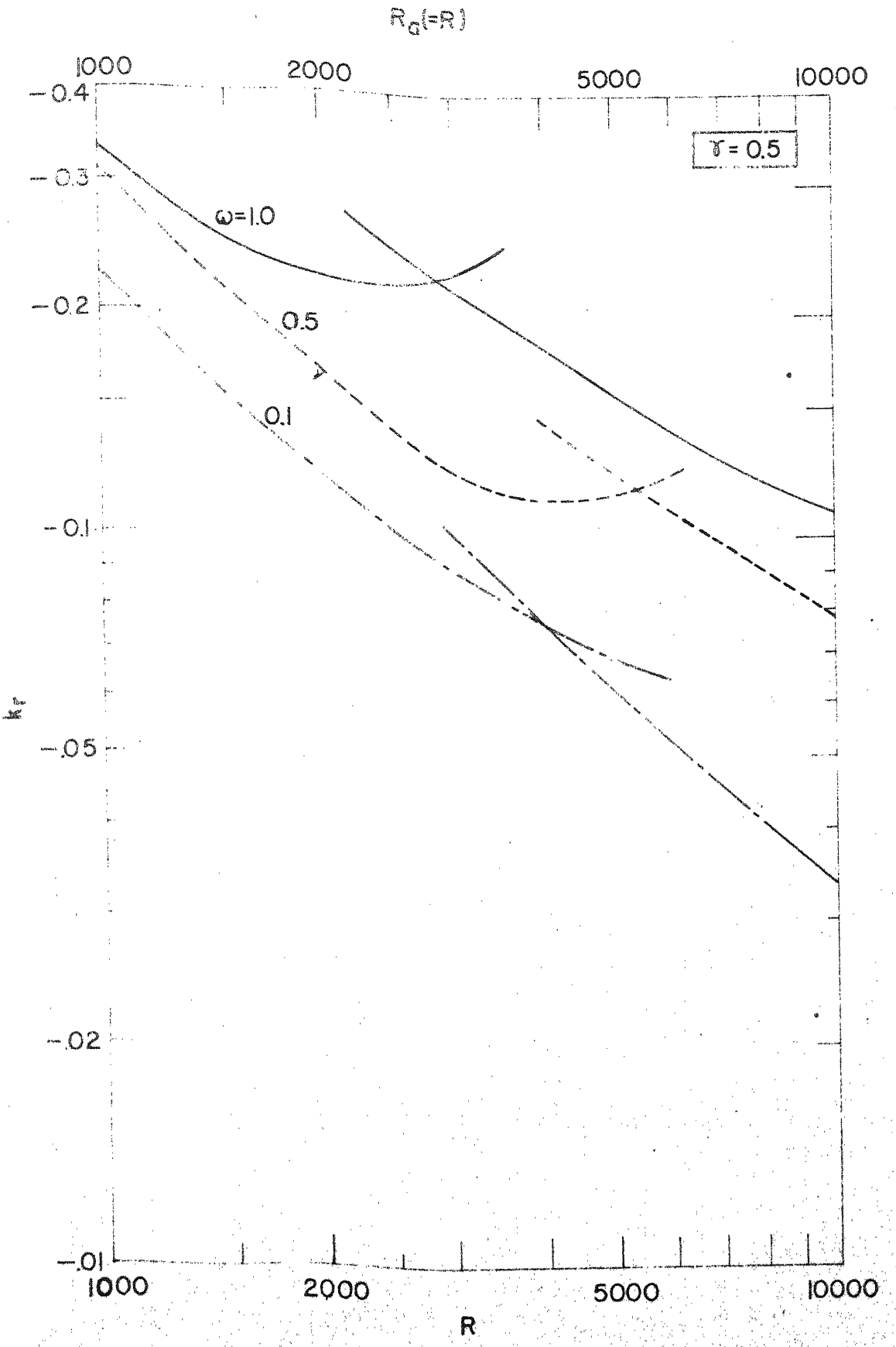

Figure 4.3 Variation of k_r with R for the Least Stable Mode for Different ω.

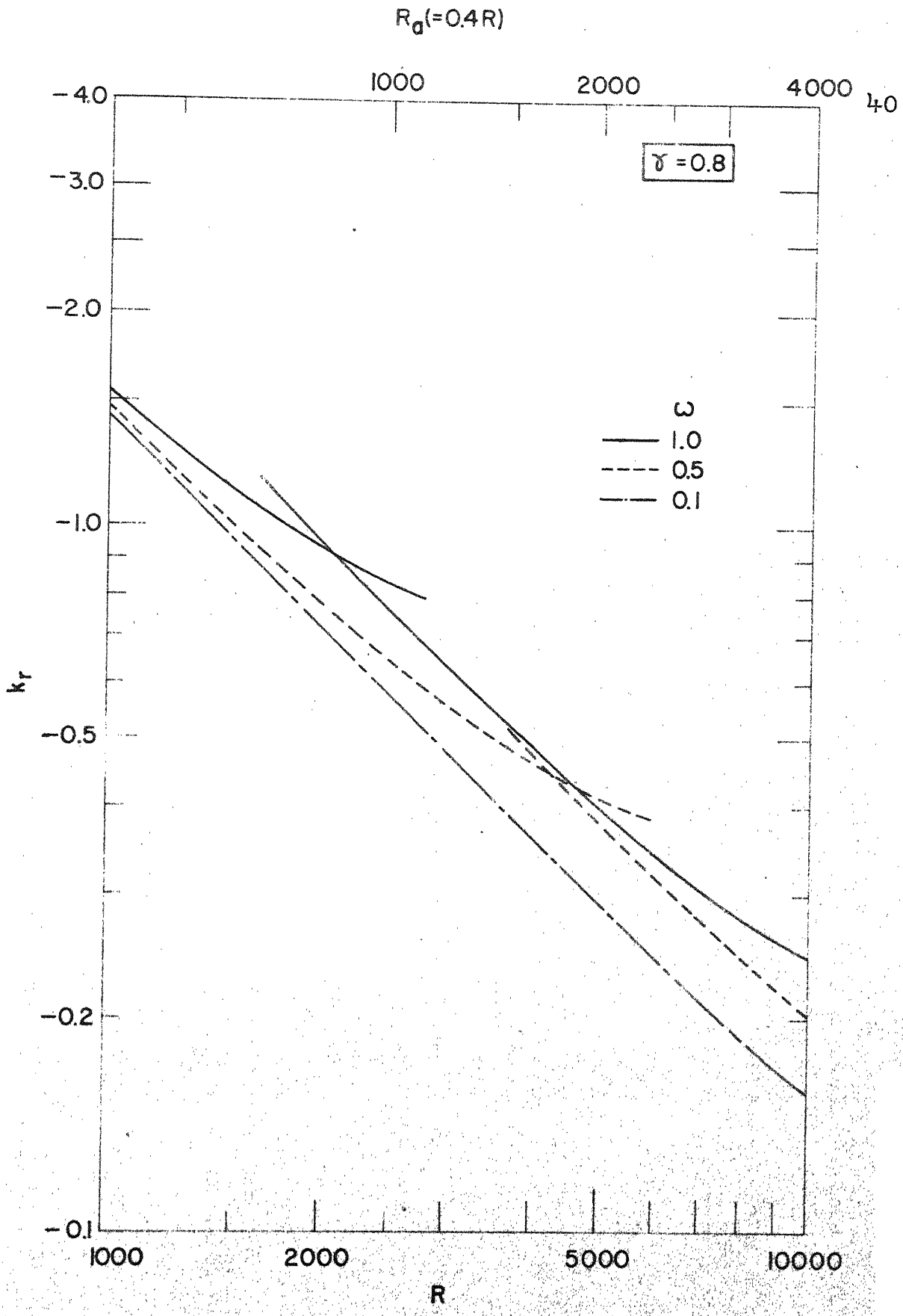

Figure 4.4 Variation of k_r with R for the Least Stable Mode for Different ω.

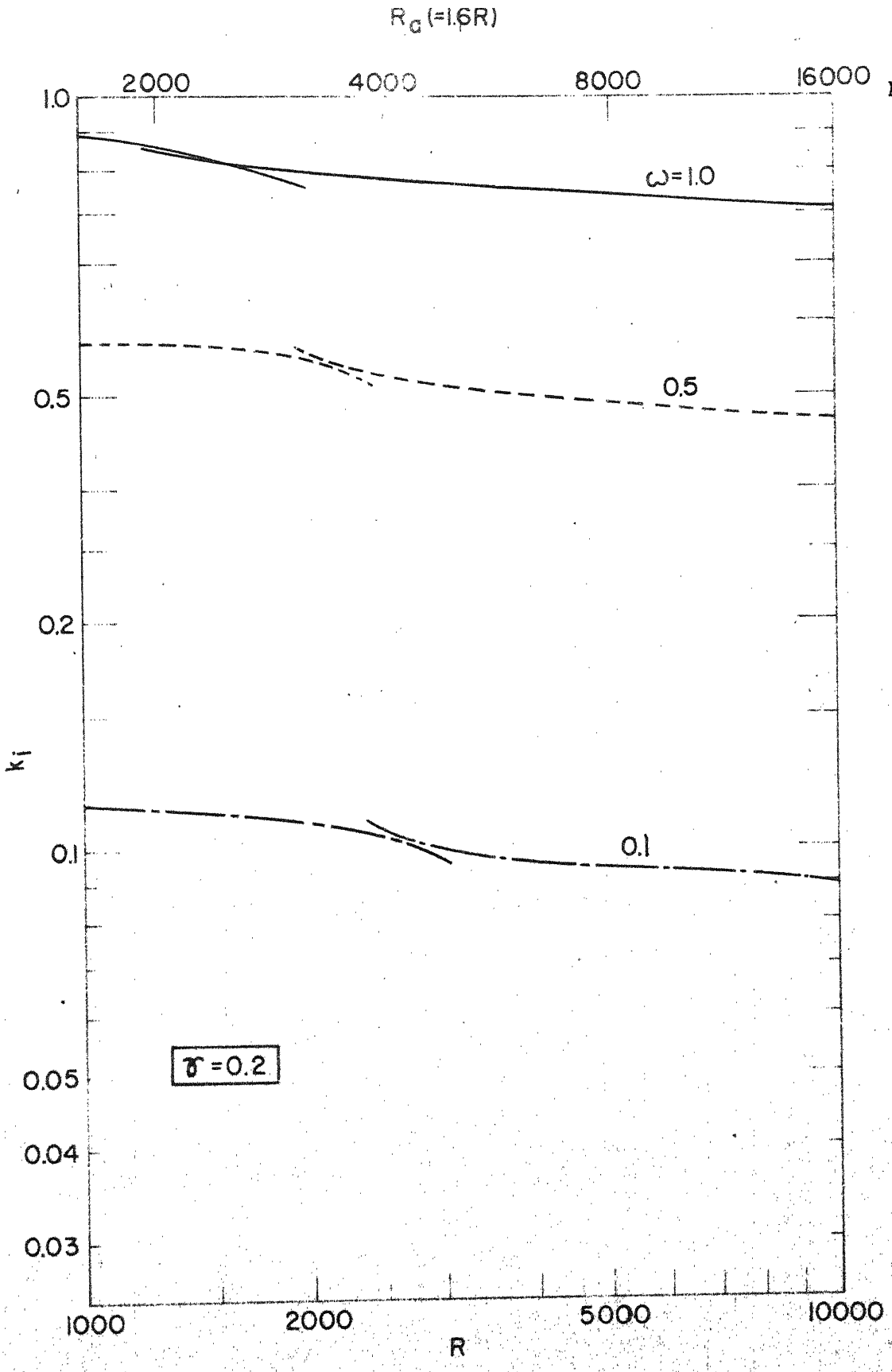

Figure 4.5 Variation of k_i with R for the Least Stable Mode for Different ω.

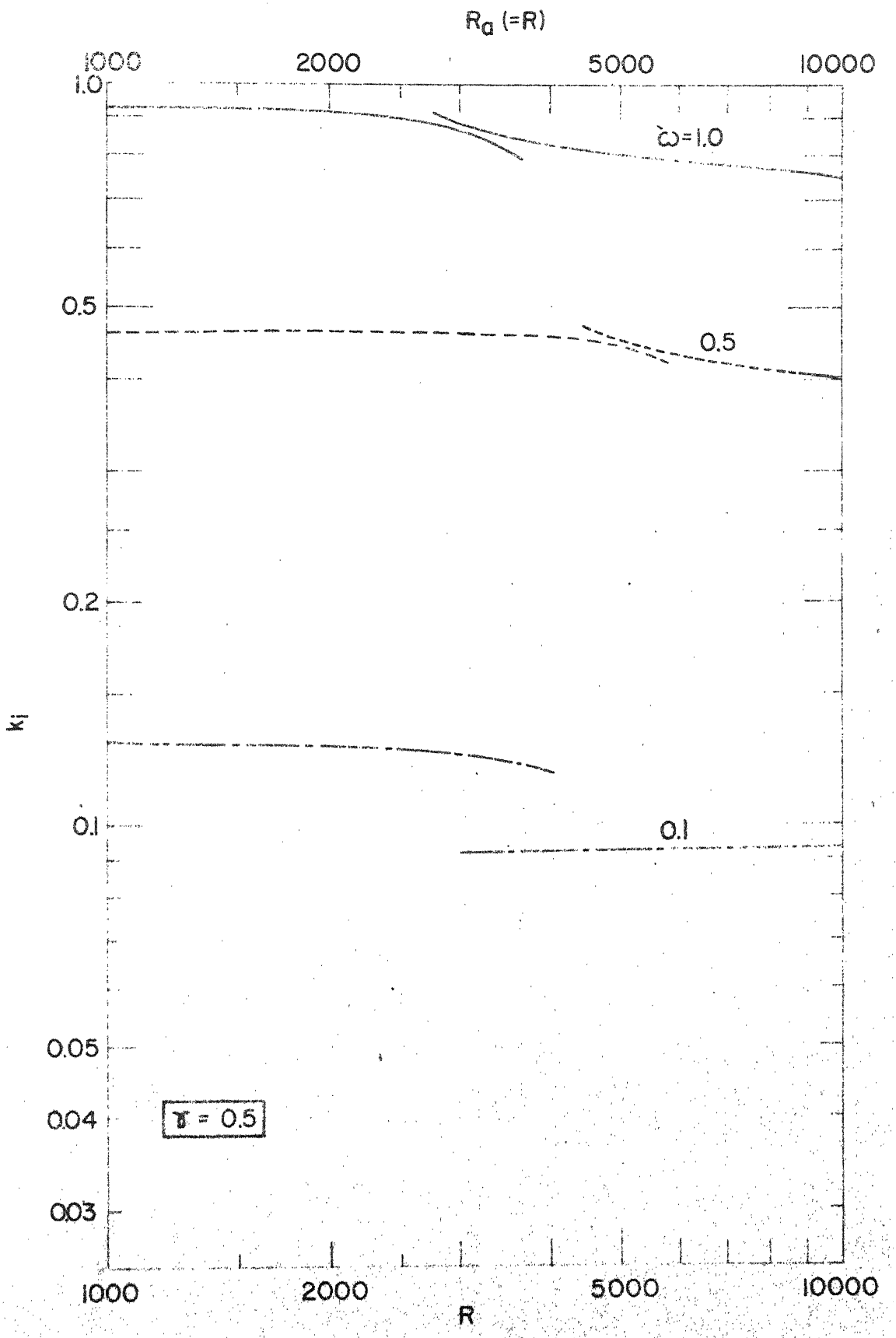

Figure 4.6 Variation of k_i with R for the Least Stable Mode for Different ω.

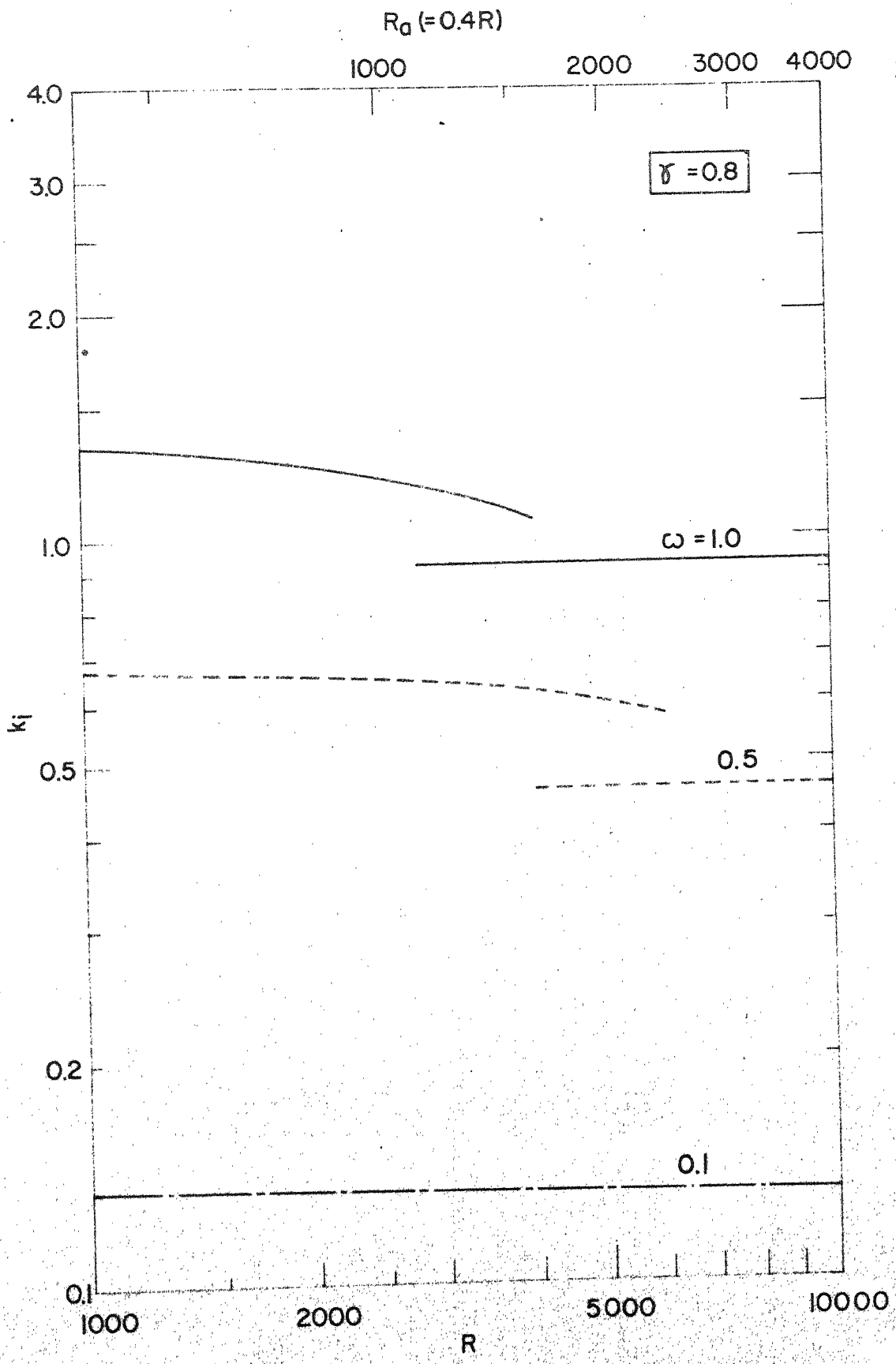

Figure 4.7 Variation of k_i with R for the Least Stable Mode for Different ω.

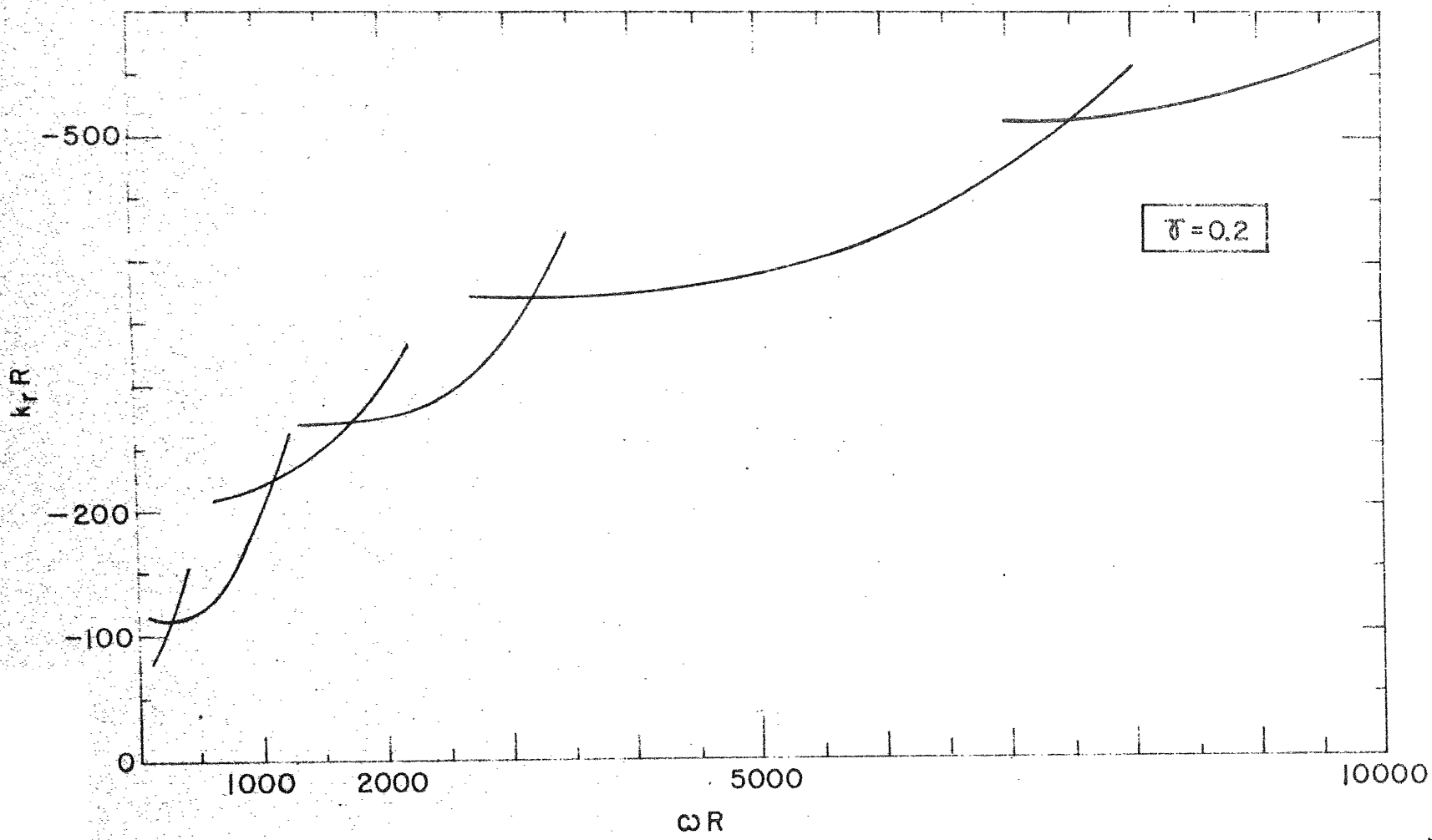

Figure 4.8 Variation of $k_r R$ with ωR for the Least Stable Mode.

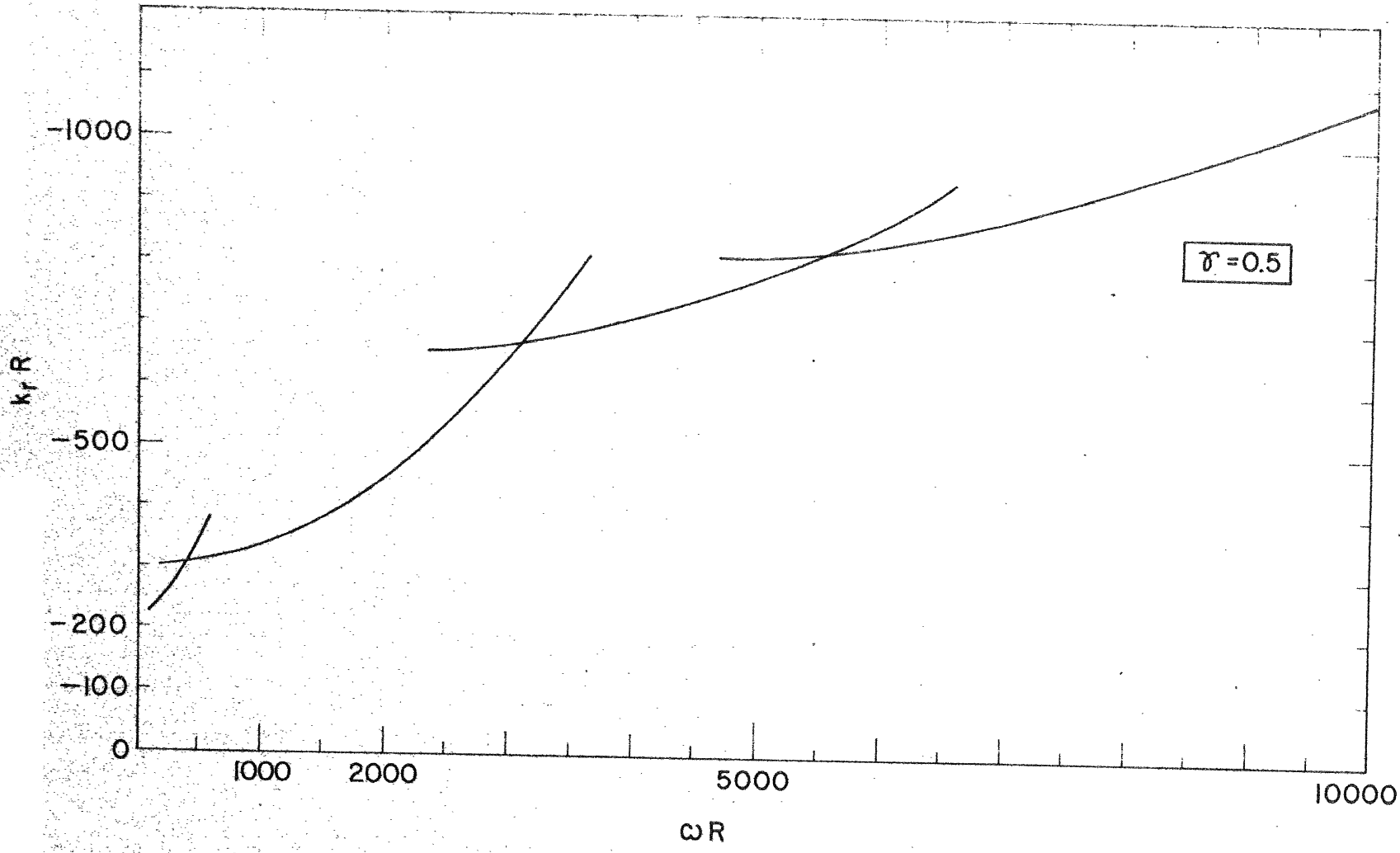

Figure 4.9 Variation of $k_r R$ with ωR for the Least Stable Mode.

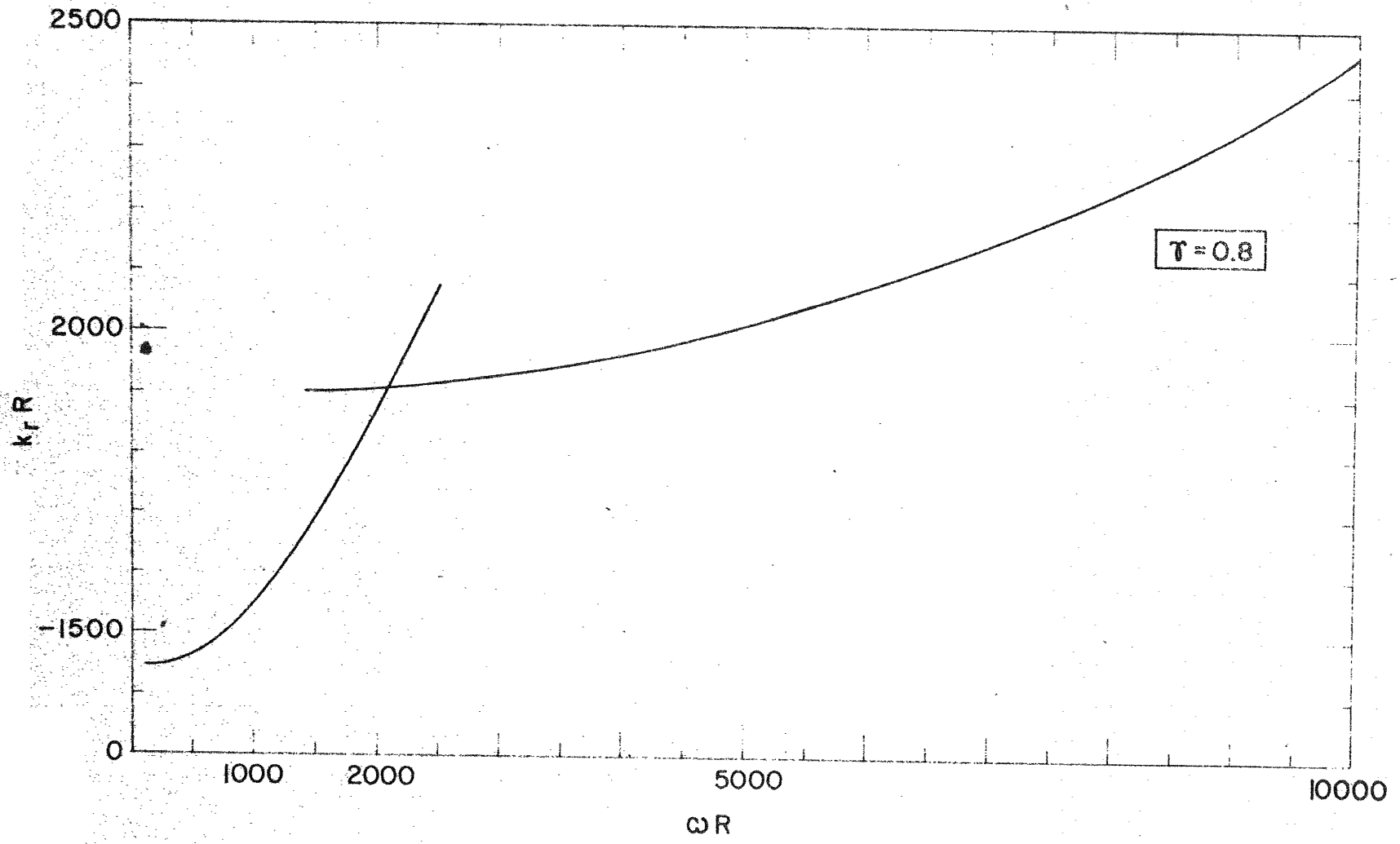

Figure 4.10 Variation of $k_r R$ with ωR for the Least Stable Mode.

TABLE 4-1

Eigenvalues for the Least Stable Mode and for some Other Stable Modes (γ = 0.2)

S.No.	ω	R	R_a	Least Stable Mode			Other Stable Modes		
				k_r	k_i	C_p	k_r	k_i	C_p
1	0.1	1,000	1,600	-0.07824	0.11477	0.87129	-0.11651	0.08684	1.15152
2	0.1	2,000	3,200	-0.04836	0.10819	0.92423	-0.06253	0.08809	1.13513
3	0.1	4,000	6,400	-0.02921	0.09563	1.04561	-0.03962	0.08600	1.16276
4	0.1	6,000	9,600	-0.02167	0.09328	1.07193	-0.03045	0.08268	1.20947
5	0.1	8,000	12,800	-0.01980	0.09208	1.08600			
6	0.1	10,000	16,000	-0.02049	0.08935	1.11916			
7	0.5	1,000	1,600	-0.12190	0.47062	1.06241			
8	0.5	2,000	3,200	-0.10228	0.44672	1.11925	-0.11144	0.39836	1.25508
9	0.5	4,000	6,400	-0.06934	0.39745	1.25802	-0.07586	0.37846	1.32113
10	0.5	6,000	9,600	-0.05493	0.38347	1.30388			
11	0.5	8,000	12,800	-0.04702	0.37515	1.33278			
12	0.5	10,000	16,000	-0.04171	0.36950	1.35315	-0.04501	0.35993	1.38914
13	1.0	1,000	1,600	-0.20339	0.89321	1.11956			
14	1.0	2,000	3,200	-0.13837	0.79498	1.25788	-0.15154	0.75707	1.32088
15	1.0	4,000	6,400	-0.09393	0.75033	1.33275			
16	1.0	6,000	9,600	-0.07557	0.73080	1.36836	-0.08137	0.71431	1.39995
17	1.0	8,000	12,800	-0.06485	0.71942	1.39000	-0.07170	0.71528	1.39804
18	1.0	10,000	16,000	-0.05765	0.71175	1.40497			

TABLE 4-2

Eigenvalues for the Least Stable Mode and for some Other Stable Modes (γ = 0.5)

S.No.	ω	R	R_a	Least Stable Mode			Other Stable Modes		
				k_r	k_i	C_p	k_r	k_i	C_p
1	0.1	1,000	1,000	-0.22500	0.12910	0.77456			
2	0.1	2,000	2,000	-0.12104	0.12687	0.78817	-0.15111	0.09120	1.09638
3	0.1	4,000	4,000	-0.07684	0.11872	0.84227	-0.07701	0.09189	1.08814
4	0.1	6,000	6,000	-0.05252	0.09240	1.08224	-0.06336	0.10656	0.93839
5	0.1	8,000	8,000	-0.04040	0.09268	1.07892			
6	0.1	10,000	10,000	-0.03334	0.09278	1.07779			
7	0.5	1,000	1,000	-0.31139	0.46077	1.08514			
8	0.5	2,000	2,000	-0.16675	0.46384	1.07795	-0.22331	0.46459	1.07620
9	0.5	4,000	4,000	-0.11200	0.46055	1.08565			
10	0.5	6,000	6,000	-0.10787	0.43229	1.15663			
11	0.5	8,000	8,000	-0.08999	0.41231	1.21267	-0.18903	0.45730	1.09337
12	0.5	10,000	10,000	-0.07781	0.40241	1.24251	-0.16583	0.44522	1.12303
13	1.0	1,000	1,000	-0.33358	0.92724	1.07846			
14	1.0	2,000	2,000	-0.22379	0.92079	1.08602	-0.27382	0.85399	1.17096
15	1.0	4,000	4,000	-0.17983	0.82467	1.21260			
16	1.0	6,000	6,000	-0.13894	0.79180	1.26294	-0.14463	0.77493	1.29043
17	1.0	8,000	8,000	-0.11746	0.77422	1.29161	-0.12208	0.76048	1.31495
18	1.0	10,000	10,000	-0.10746	0.75073	1.33203			

TABLE 4-3

Eigenvalues for the Least Stable Mode and for some Other Stable Modes (γ = 0.08)

S.No.	ω	R	R_a	Least Stable Mode			Other Stable Modes		
				k_r	k_i	C_p	k_r	k_i	C_p
1	0.1	1,000	400	-1.44639	0.13467	0.74253			
2	0.1	2,000	800	-0.72167	0.13328	0.75029			
3	0.1	4,000	1,600	-0.36380	0.13274	0.75334			
4	0.1	6,000	2,400	-0.24621	0.13232	0.75572			
5	0.1	8,000	3,200	-0.18855	0.13179	0.75873			
6	0.1	10,000	4,000	-0.15483	0.13113	0.76256			
7	0.5	1,000	400	-1.47152	0.67160	0.74448			
8	0.5	2,000	800	-0.77440	0.65819	0.75965			
9	0.5	4,000	1,600	-0.46690	0.62809	0.79605	-0.47562	0.46072	1.08525
10	0.5	6,000	2,400	-0.32141	0.46093	1.08474	-0.38236	0.57791	0.86518
11	0.5	8,000	3,200	-0.24561	0.46106	1.08444	-0.32534	0.52652	0.94962
12	0.5	10,000	4,000	-0.20126	0.46114	1.08426	-0.27690	0.49407	1.01198
13	1.0	1,000	400	-1.54976	1.33260	0.75040			
14	1.0	2,000	800	-0.93346	1.26274	0.79192	-0.95115	0.92133	1.08539
15	1.0	4,000	1,600	-0.49120	0.92206	1.08452	-0.65186	1.05390	0.94885
16	1.0	6,000	2,400	-0.34541	0.92229	1.08426	-0.48037	0.95040	1.05219
17	1.0	8,000	3,200	-0.27922	0.92204	1.08455			
18	1.0	10,000	4,000	-0.24608	0.92090	1.08589			

CHAPTER 5

CONCLUSIONS

The effect of modified Reynolds number R, diameter ratio γ , and frequency ω on the relative stability of concentric annular flow and on the wavelength of the disturbance can be summarized as follows:

(i) For a fixed γ and ω , the least stable mode becomes less stable and has a larger wavelength as R is increased.

(ii) For a fixed γ and R, the least stable mode becomes less stable and has a larger wavelength as ω is decreased.

(iii) For a fixed ω and R, the least stable mode becomes less stable and has a larger wavelength as γ is decreased.

On the basis of these results, it is concluded that up to a modified Reynolds number of 10,000, the concentric annular flow is spatially stable to infinitesimal axisymmetric disturbances. These results are in conformity with those of Mott and Joseph for the temporal stability [6].

APPENDIX I

STEP-BY-STEP INTEGRATION TECHNIQUE

The fourth order Runge-Kutta method used for the step-by-step integration of the coupled differential equations (3.22) through (3.25) is given in a tabular form here. Tables AI-1 and AI-2 exhibit the appropriate formulae for first and second order differential equations. In these tables h is the step size, D is the operator d/dx, and x_o, y_o and Dy_o are the values known at the starting point of the integration step. The procedure is to calculate K_1 first and then go to the first column in the second row. After calculating K_2 by traversing the second row from left to right, we go to the first column in the third row, and so on till K_4 is calculated. The factors in the 'Correction' column are then calculated before we go to fifth row; x_1, y_1 and Dy_1 are the values at the end of the present step, that is they are the starting point values for the next integration step. The whole procedure is, therefore, repeated for successive steps.

TABLE AI - 1

Runge-Kutta Scheme for Differential Equations of the First Order; $Dy = f(x,y)$

x	y	$K_m = hf(x,y)$	Correction
x_o	y_o	K_1	
$x_o + \frac{1}{2} h$	$y_o + \frac{1}{2} K_1$	K_2	
$x_o + \frac{1}{2} h$	$y_o + \frac{1}{2} K_2$	K_3	
$x_o + h$	$y_o + K_3$	K_4	$K = \frac{1}{6} (K_1 + 2K_2 + 2K_3 + K_4)$
$x_1 = x_o + h$	$y_1 = y_o + K$		

TABLE AI - 2

Runge-Kutta Scheme for Differential Equations of the Second Order; $D^2y = f(x,y,Dy)$

x	y	Dy	$K_m = \frac{h^2}{2} f(x,y,DY)$	Correction
x_o	y_o	Dy_o	K_1	
$x_o + \frac{1}{2} h$	$y_o + \frac{1}{2} h\, Dy_o + \frac{1}{4} K_1$	$Dy_o + K_1/h$	K_2	
$x_o + \frac{1}{2} h$	$y_o + \frac{1}{2} h\, Dy_o + \frac{1}{4} K_1$	$Dy_o + K_2/h$	K_3	$K = \frac{1}{3} (K_1 + K_2 + K_3)$
$x_o + h$	$y_o + h\, Dy_o + K_3$	$Dy_o + 2K_3/h$	K_4	$K' = \frac{1}{3} (K_1 + 2K_2 + 2K_3 + K_4)$
$x_1 = x_o + h$	$y_1 = y_o + hDy_o + K$	$Dy_1 = Dy_o + K'/h$		

APPENDIX II

EIGENVALUE SEARCH TECHNIQUE

The eigenvalue search technique developed by Garg and Rouleau [4] uses the result of Cauchy Integral Theorem for determining the number of zeros of a complex function in any closed region of the argument in which the function is analytic.

For a function f(z), analytic except for poles in the interior of a closed curve C on the z-plane, and for f(z) and Df(z) continuous on C, the residue theorem gives

$$Z - P = \frac{1}{2\pi i} \int_C \frac{Df(z)}{f(z)}\, dz \,, \qquad \text{(AII.1)}$$

where Z and P denote respectively the number of zeros and the number of poles of f(z) within the closed region C (counted with their multiplicities), and where D is the operator d/dz. Since Df(z)/f(z) is the derivative of ln [f(z)], to calculate the definite integral the right-hand side of equation (AII.1), it is sufficient to know only the variation of

$$\ln |f(z)| + i \text{ angle } [f(z)]$$

when the variable z describes the contour C in the positive sense, that is, in the counter-clockwise sense. But |f(z)| returns to its initial value, while the angle of f(z) increases by $2\pi M$, M being either zero or a

positive or negative integer. Thus equation (AII.1) reduces to

$$Z - P = \frac{2\pi Mi}{2\pi i} = M; \qquad \text{(AII.2)}$$

that is, the difference (Z-P) is equal to the integer quotient obtained by dividing the variation of the angle of f(z) by 2π as the variable z describes the boundary C in the positive sense.

The function f(z) can be expressed in terms of its real and imaginary parts as follows

$$f(z) = X + iY.$$

Then, as the point z = x + iy describes the curve C in the positive sense, the point whose coordinates are (X, Y) with respect to a system of rectangular axes with the same orientation as the first system, describes also a closed curve C_1, and it is only required to count the number of revolutions which the radius vector joining the origin of coordinates to the point (X, Y) has turned through in one sense or the other. There is thus no need of plotting the actual curve C_1. Instead, the integer M is given by the net multiples of 2π by which the phase angle of f(z) changes in going round the curve C_1. When the point z describes the curve C in the positive sense, any counterclockwise movement of the phasor for f(z) is considered positive while the clockwise movement is considered negative.

In application to this problem, each element of the determinant (equation (3.31)) is a function of the complex eigenvalue k or ω. In fact, the determinant det can be considered as some high order polynomial in the eigenvalue due to the recurrence relations for the coefficients in the series solution of the stability equations. Therefore, the function det (k) or det (ω) has no poles, that is, $P \equiv 0$ in equations (AII.1) and (AII.2), and $Z = N$. Thus, the problem of finding the number of eigenvalues within a closed region of the complex k or ω-plane is as simple as counting the net multiples of 2π by which the phase angle of the determinant changes as k or ω assumes values on the closed contour in the complex plane.

This method can also be used to provide a close approximation to the true eigenvalue so that an iterative technique may converge to it. If it so happens that the closed contour chosen on the complex k or ω-plane passes close to an eigenvalue within the contour at some location, the phase angle of the determinant will change by about 180° and the magnitude of the determinant will show a dip. However, depending on the closeness of the boundary to the eigenvalue, this may or may not be the case. Nevertheless, we can always subdivide the region investigated on the complex plane and thus isolate a relatively small region which contains the eigenvalue. Experience has

shown that except for the least stable mode, it is sufficient to know only two significant digits correctly in the approximate eigenvalue. The secant method used for the iterative minimization scheme then converges to the true eigenvalue easily. For the least stable mode, it is generally required to know the approximate eigenvalue to one more order of accuracy.

double precision form. Although the double precision complex arithmetic is not available on the IBM 7044 system it was created out of necessity. Thus, every double precision complex variable was expressed in terms of two double precision variables which represent the real and imaginary parts of the complex quantity.

ME-1976-M-AGA-LIN